

A review of oxygen-17 solid-state NMR of organic materials—towards biological applications

V. Lemaître,^{a,b} M.E. Smith,^c and A. Watts^{a,*}

^a *Biomembrane Structure Unit, Department of Biochemistry, Oxford University, South Parks Road, Oxford OX1 3QU, UK*

^b *Nestec S.A., BioAnalytical Department, Vers-Chez-Les-Blanc, CH-1000 Lausanne 26, Switzerland*

^c *Department of Physics, University of Warwick, Coventry CV4 7AL, UK*

Received March 8, 2004; revised March 31, 2004

Abstract

¹⁷O solid state NMR of organic materials is developing rapidly. This article provides a snapshot of the current state of development of this field. The NMR techniques and enrichment protocols that are driving this progress are outlined. The ¹⁷O parameters derived from solid-state NMR experiments are summarized and the structural sensitivity of the approach to effects such as hydrogen bonding highlighted. The prospects and challenges for ¹⁷O solid-state NMR of biomolecules are discussed.

© 2004 Elsevier Inc. All rights reserved.

Keywords: Oxygen-17; Solid-state NMR; MAS; DOR; DAS; MQMAS; Amino acids; Organic molecules; Peptide; Hemeprotein; Hydrogen-bond; Biological applications; Review

1. Introduction

In the last 10 years, the efforts to exploit oxygen-17 (¹⁷O) in solid-state NMR have greatly increased, with applications ranging from studies of amorphous materials [1–7], zeolites [8,9] and minerals [10–12] to polymers [13,14]. Although ¹⁷O is still a relatively exotic nucleus for NMR study, the field has now matured to such a stage where applications of the techniques to problems of real biological significance are close to being realized.

The use of quadrupolar nuclei, in general, in biological systems was reviewed in 1998 [15]. Here, we review the variety of NMR approaches for studying ¹⁷O in systems of biological interest, such as organic molecules, amino acids and peptides. The different systems studied, the techniques applied and the results obtained will be discussed.

2. Perspective and overview

One of the main reasons for studying oxygen is its ubiquity in biology. Indeed, oxygen controls or participates in nearly every biological process, especially those involving aerobic metabolism. Oxygen occupies a key position both at the structural and physiological level. In all macromolecules, including peptides, proteins, DNA and RNA (especially ribosome) and carbohydrates, oxygen has a major role in the molecular conformation observed, such as the secondary, tertiary and quaternary structure. In proteins that are stabilized through multiple hydrogen bonds, changes which occur between ground and transition states can also induce an important effect on enzyme catalysis [16]. It is therefore not a surprise that oxygen atoms are involved in triggering, signalling and activation mechanisms. Many physiological processes, like substrate–enzyme, drug–receptor or protein–protein interactions, imply non-covalent bonding between the substrates. Taking into account the great importance of hydrogen bonding in biological systems, oxygen-17 has the potential of being a valuable probe of both structure and function.

*Corresponding author. Tel.: +44-1865-275268; fax: +44-1865-275234.

E-mail address: anthony.watts@bioch.ox.ac.uk (A. Watts).

^{17}O is the only NMR-active oxygen isotope (nuclear spin = $\frac{5}{2}$) and its application in NMR has been hindered by several of its intrinsic nuclear properties resulting in low sensitivity and complex spectra. Amongst these are (1) the small gyromagnetic ratio $\gamma = -3.6279 \times 10^7 \text{ rad T}^{-1} \text{ s}^{-1}$ (comparable to ^{15}N), so that the resonance frequency is about $\frac{1}{7}$ th that of protons (54.221 MHz at 9.39 T which is 400 MHz for ^1H), giving a relative sensitivity of 1.830 (relative to ^{13}C at constant field for equal numbers of nuclei [17]); (2) a low natural abundance of 0.037% leading to an absolute sensitivity of 0.0611 (compared to ^{13}C) so that isotopic enrichment is usually necessary; (3) a nuclear quadrupole moment $Q = 2.558 \times 10^{-30} \text{ m}^2$ (significant but much smaller than many other nuclei, e.g. ^{27}Al); and (4) in a number of cases a large electric field gradient (EFG) is experienced. As a non-integer quadrupolar nucleus it is usually the central ($\frac{1}{2}, -\frac{1}{2}$) transition that is observed and the quadrupolar effects have to be considered beyond first order [3]. This further reduces the sensitivity compared to spin- $\frac{1}{2}$ nuclei and in solids it is the residual second-order quadrupolar broadening for half-integer spin quadrupolar nuclei that usually determines the line widths in magic angle spinning experiments (MAS) (see [18] and references therein). However compared to ^{27}Al in sites of comparable distortion second-quadrupole effects lead to only 0.064 as much broadening [18]. ^{17}O exhibits a large NMR chemical shift range depending on the chemical function and the local environment [3], with the shift being distributed around ~ 2000 ppm (from water to dioxygen [19]).

As a quadrupolar nucleus, oxygen is sensitive to both the EFG and chemical shift anisotropy (CSA), which are anisotropic NMR interactions that can be used as probes for characterizing the local environment of the nucleus. The advantage of exploiting such anisotropic interactions (2nd rank tensors) is that they are able to provide three-dimensional information about the local electronic structure. Indeed, both these parameters have been shown to be very sensitive to local structure and bonding (including hydrogen bonding). Anisotropic bonding of oxygen atoms in many solids produces strong electric field gradients at the oxygen nuclei and quadrupole coupling constants χ_Q of several MHz. The average for the quadrupole constant is 4.2 ± 1.5 MHz in inorganic material (average based on about 300 values [3,20]). This implies, that for ^{17}O , the quadrupolar interaction is likely to be dominant, although other nuclear spin interactions such as dipolar interactions ($\sim 10^4$ Hz) and CSA (~ 10 – 10^4 Hz) cannot be neglected. As even higher magnetic fields are applied the CSA will become increasingly important.

In 1981, it was already suggested that both EFG and CSA would be very sensitive to the electronic structure of the molecule and that they could potentially yield details and degrees of resolution [21] not available from

X-ray or neutron diffraction. Amongst these structural details, are molecular dynamics, and inter- and intra-molecular interactions such as hydrogen bonds. Small energy changes in the electronic structure cannot be detected by diffraction methods alone [22], because of the character of the irradiation inherent to these methods, and the inherent diffuse nature of electronic distributions which are not sufficiently resolved. It is more than 20 years since this statement was made, and since then very significant improvements in both experimental NMR (especially high magnetic fields with concomitant increases in sensitivity and resolution) and quantum chemical simulation have made it possible to collect accurate data in order to relate NMR parameters to chemical structure.

^{17}O solution NMR is a useful technique to solve structural problems for small organic molecules. The fast reorientation of the molecules in solution (fast tumbling rate, $\tau_r > Q^{-1} \sim 10^{-6}$ – 10^{-7} s [19]) results in narrow spectral lines due to the averaging of the quadrupolar interaction. Rapid quadrupolar relaxation of ^{17}O has, however, prevented successful applications of solution ^{17}O NMR to biological macromolecules [19]. The large quadrupolar interaction of oxygen-containing functional groups can cause highly effective relaxation, which leads to strong broadening of the NMR signals, which can be severe for large molecules. ^{17}O solid-state NMR has therefore been seen as an alternative for structural studies to ^{17}O solution NMR [23], since the relaxation times are much longer and the intrinsic spectral resolution is not limited by molecular weight.

3. General background of experimental solid-state NMR techniques applied for half-integer spin quadrupolar nuclei

A whole range of NMR techniques can be applied to half-integer spin quadrupolar nuclei (such as ^{17}O) in solid materials including static, magic angle spinning (MAS) and higher-order averaging techniques. Static experiments are usually performed at several different magnetic fields, or in conjunction with MAS, to enable all the tensor properties of the ^{17}O sites present to be determined. The limitation of static work is the inherent resolution when dealing with resonance lines that can be very broad, up to 100 kHz wide from some amino acids [24]. Hence in complex molecules with different oxygen sites there can be strong overlap between the different resonances.

High-resolution (or at least higher resolution) ^{17}O solid-state NMR has been made possible through the application of MAS (see Fig. 1 for an illustration). However, the angular variation of the second-order quadrupolar interaction is more complex than ($3 \cos^2 \theta - 1$) so that this interaction is incompletely averaged under MAS. One of the most immediate

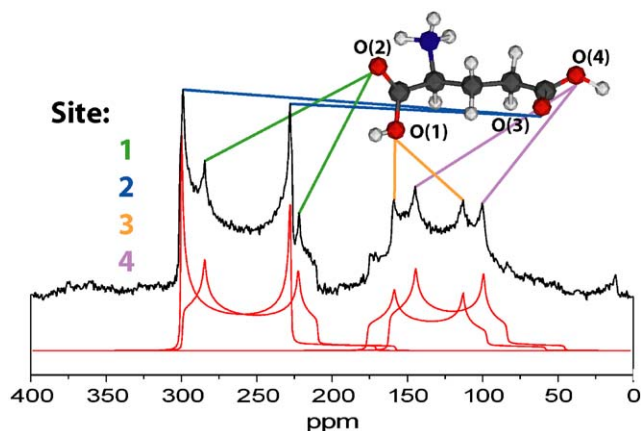


Fig. 1. ^{17}O MAS NMR of L-glutamic acid · HCl. Resolution of the four distinct crystallographic oxygen sites. A highly structured spectrum is observed with 2 main resonances centred at ~ 260 and 125 ppm. Each resonance is composed of 2 strongly overlapping lines. The structure on the resonance at lower shift only became clear when high ^1H -decoupling powers were used (adapted from [35] with permission of the copyright owner).

consequences of this is that the residual line widths under MAS (since spinning by MAS only narrows a factor of ~ 3.6 compared to a static sample [25]) means that the resolution improvement due to MAS is not as good as it would be for a spin- $\frac{1}{2}$ system, and often MAS of amino acids leads to resonances that are 10–12 kHz wide. Therefore more complex averaging techniques are required to acquire ^{17}O spectra with higher resolution.

Two main avenues have been explored to average the second-order quadrupolar broadening as well as first-order effects: extended mechanical averaging of the sample (DOR [26–28], DAS [29,30]) or a combination of multiple-quantum excitation effectively averaging in spin space and fast spinning (MQMAS) [31]. MQMAS is a two-dimensional (2D) sequence that correlates multiple quantum signal with that of the central transition. In the 2D data set there exists directions where both the first- and second-order quadrupole broadening are removed to produce the high resolution. An alternative high resolution approach for half-integer quadrupole nuclei is satellite transition MAS [32,33]. This correlates single quantum signal from the satellite and central transitions in a 2D data set, from which it is again possible to produce an isotropic high-resolution spectrum. The references given here provide more details about the physical background and implementation of these techniques, and they have been reviewed in detail previously [18].

The advantages of these techniques are illustrated by MQMAS which reduces the width in the isotropic F1 dimension, and DOR which reduces the width of the NMR spectra by almost an order of magnitude, when compared to a 1D MAS NMR spectrum [34]. As an example L-monosodium glutamate (L-MSG) is shown

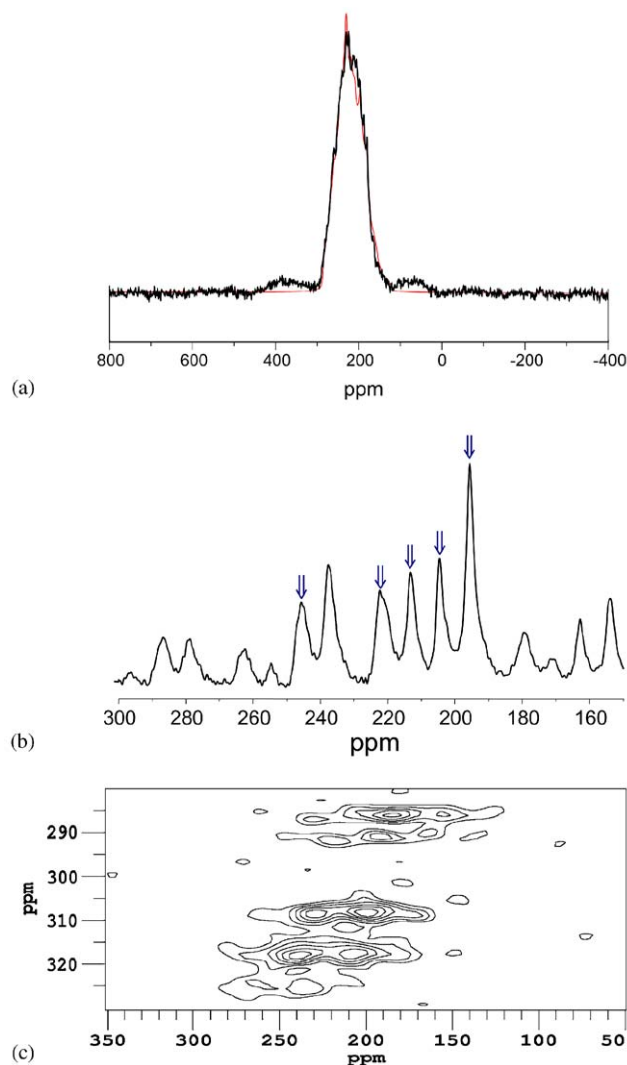


Fig. 2. 14.1 T ^{17}O NMR spectrum of L-Monosodium glutamate (a) MAS together with a simulation based on the 5 components deduced from the higher resolution data. (b) DOR (\downarrow indicate the centrebands) and (c) the centreband of the 14.1 T 3Q MAS NMR data (adapted from [35] with permission of the copyright owner).

(Fig. 2). These are the least 5 signals but in MAS spectrum there is considerable overlap. However, the additional narrowing provided by both DOR and MQ approaches gives complete resolution of the different signals [35]. The main contribution to the residual line width is then probably incomplete removal of the ^1H - ^{17}O dipolar interactions (this can possibly be improved by using the two-pulse phase modulation (TPPM) [36] for better dipolar ^1H decoupling [34]). In MQMAS, the line width is not limited by the molecular weight of the system under observation [34]. MQMAS can also suffer problems at high spinning rates and larger quadrupole interactions due to excitation effects of the MQ transitions. Consequences of this can be that sites that are unequally excited so that MQ spectra

cannot really be used for quantification ([18] and references therein).

A comparison of DOR and MQMAS techniques for an inorganic sample, shows the line widths of the ^{17}O DOR NMR spectra are narrower than for ^{17}O 3QMAS NMR by a factor of two [37].

DOR has advantages over MQMAS in that no sensitivity is lost in the signal acquisition (in fact sensitivity is gained since the signals are narrower) and it is a 1D technique. The main disadvantage of DOR is that a highly specialized probehead is required. There have been continued improvements in the maximum rotation rates of the outer rotor. Current maximum rates are ~ 2 kHz, which means that with odd-order sideband suppression [28], sidebands are separated by ~ 4 kHz. Although still large numbers of sidebands can be produced they can be handled and the much improved resolution would allow several different sites in the same sample to be resolved in the DOR spectrum.

The advent of higher magnetic fields, faster magic angle spinning (MAS) and the introduction of techniques to improve the spectral resolution has seen a significant increase in ^{17}O NMR reports from inorganic materials. The resonances are narrower at higher applied magnetic fields because of the inverse dependence of the second-order quadrupolar broadening on the applied magnetic field (\propto to B_0^2 in ppm). Progress in ^{17}O solid-state NMR applied to biological sciences has been much more limited since ^{17}O NMR from organic materials presents an even greater challenge because typically much greater quadrupole interactions are experienced in such materials. Fig. 3 summarizes some of the milestones achieved during the last 20 years regarding mainly the study of organic and biologically related molecules with ^{17}O solid-state NMR, showing the relatively slow progress until the last 5 years.

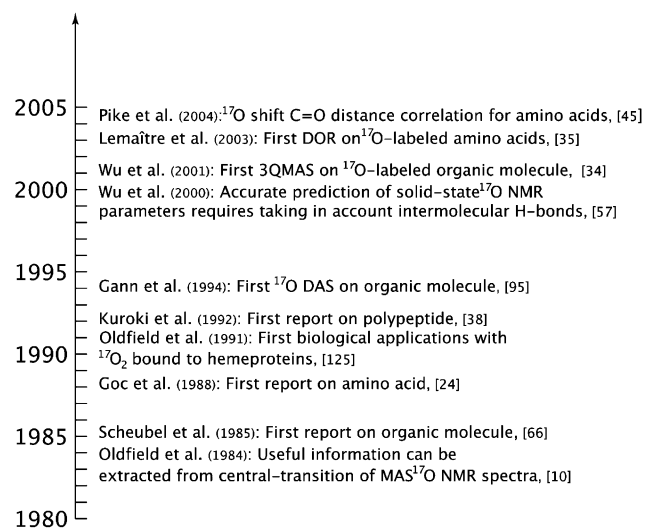


Fig. 3. Important milestones in the application of solid-state ^{17}O NMR to organic molecules and related materials.

^{17}O solid-state NMR has already developed sufficiently that it is able to resolve simultaneously several oxygen sites, even if they are chemically very similar. For example, MAS experiment provides enough resolution to observe and characterize the four oxygen atoms from crystalline L-glutamic acid (Fig. 1). DOR experiments provide even better resolution with all the 5 sites in L-MSG resolved (Fig. 2). The increase in the resolution will allow the study of more complex molecules, perhaps even uniformly labelled peptides and more complex organic molecules.

Recent reports of ^{17}O NMR from organic materials have included O_2 and CO interacting with hemeproteins, polymers, various crystalline organic molecules, amino acids and nucleic acid bases—these applications will be reviewed here.

4. Sample preparation

^{17}O solid-state NMR requires selective isotopic enrichment of the sample. However, even low enrichment levels are enough to provide a sufficient increase in signal to determine the NMR parameters of the enriched sites. The lowest enrichment used for ^{17}O of organic molecules reported for NMR study is 6 at% [38–40]. Considering the current magnetic fields and probes available, and in order to ensure acquisition in a reasonable amount of time, a minimum enrichment of 10–15 at% for crystals of organic molecules is recommended. For non-crystalline organic phases, higher enrichments are preferable (minimum 40 at%).

Although it is not necessary to calculate very accurately the enrichment in ^{17}O , it is possible to monitor the enrichment using electron ionization mass spectrometry (EI-MS). As an example, Fig. 4 shows the change in the mass spectrum upon enrichment in the case of L-glutamic acid, where enrichment was carried out using 18%- ^{17}O -water. Upon enrichment, one observes an increase of the intensity of the peaks located at $M + 1$, $M + 2$, $M + 3$ and $M + 4$, where M is the molecular peak. This indicates an overall isotopic enrichment of the molecule (in this case, L-Glutamic acid has four oxygen sites). Although the level of enrichment could be higher, this level of enrichment of the water is enough to give a sample suitable for solid-state NMR studies.

The main precursors for ^{17}O enrichment are ^{17}O -water, ^{17}O -dioxygen (O_2 gas) or ^{17}O -carbon monoxide. For more information related to synthetic methods, see the review written by Butler [41] or refer directly to publications related with the solid-state NMR study where the individual enrichment schemes employed are usually discussed (See Table 2 for a detailed list). Enrichment can be at specific sites or the sample uniformly labelled. All the evidence, for example from

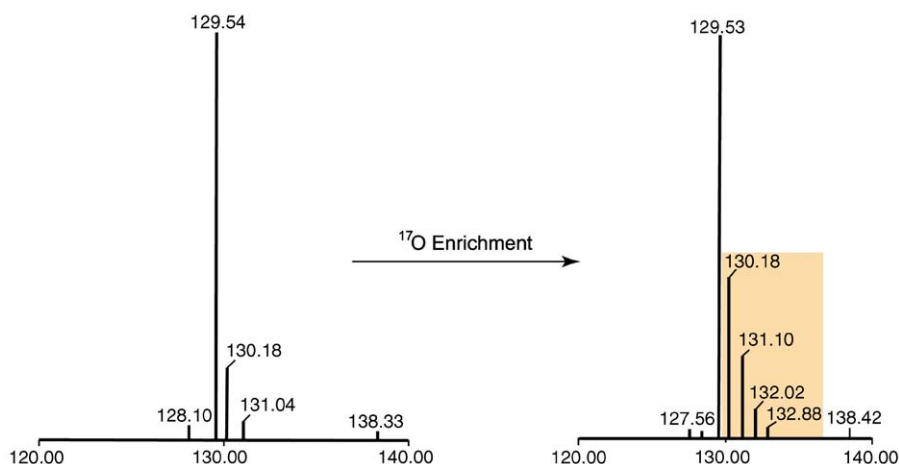


Fig. 4. Electron ionization mass spectrum of (a) L-glutamic acid and ^{17}O -enriched L-glutamic, starting with 18 at% ^{17}O -enriched water. The increase of the intensity of mass peak located at the left of the molecular peak shows that the ^{17}O enrichment was achieved.

uniformly labelled amino acids, shows that the intensity ratio between the different sites agrees exactly with the expected value.

Synthesis of ^{17}O -enriched samples can be difficult, since the number of labelled precursors on the market remains fairly limited. It is interesting to note that in 2001, the precursors commercially available were mostly limited to H_2O , O_2 and CO . As a sign of the growing interest in ^{17}O labelling, it is now possible to buy ^{17}O -enriched organic molecules such as benzophenone, phenol or even amino acids. There are now two companies providing ^{17}O labelled organic molecules (Icon Isotope Service and Cambridge Isotopes).

Enrichment of amino-acids is possible and has been described more than 20 years ago [42,43]. Synthesis of selectively enriched peptides is possible, which takes place in solution for small di- and tri-peptides [42,44]. Furthermore, solid-phase peptide synthesis (with both Boc- [42] or Fmoc-protecting groups [Lemaître et al., personal communication]) can also be performed. The enrichment of the protected amino acid can be either performed on the Boc- or MeO-protected amino acid [42] or the protection reaction (Fmoc for example) can be conducted on the amino acid without any significant loss of label [45].

5. Characteristic parameters

Generally, authors have determined as accurately and as completely as possible the NMR parameters (Table 1) characterizing the observed NMR signals. To obtain unambiguous simulations of the NMR spectra, it is usually necessary to record them at several fields (at least 2), or use a combination of methods e.g. static and MAS, DOR or MQ in order to generate enough constraints for the simulation procedure. Advances in

Table 1
NMR parameters of interest that can be extracted from ^{17}O spectra

Parameter	Symbols usually used
Isotropic chemical shift	δ_{iso}
Chemical shift anisotropy tensor (principal components in PAS)	$\sigma_{11}, \sigma_{22}, \sigma_{33}$
Orientation of CSA (euler angles)	α, β, γ
Quadrupole coupling constant	$\chi_Q = e^2qQ/h$
Nuclear quadrupolar electric moment	eQ
Quadrupolar asymmetry parameter	$\eta_Q = (q_{xx} - q_{yy})/q_{zz}$
Electric field gradient tensor (main components)	$V_{11}, V_{22}, V_{33} (=eq)$

both experimental NMR and computation of the NMR parameters have resulted in a much improved correlation between anisotropic NMR properties (EFG, CSA) and molecular structure.

Indirect spin coupling constants will not be discussed here, since there are no reports so far, for an organic molecule in ^{17}O solid-state NMR. However, this could turn out to be another very useful parameter, which might be related to structure. Relaxation properties of ^{17}O -labelled solids also need to be investigated in more detail but very wide variations in T_1 have been determined from several seconds to a few ms.

5.1. Chemical shift

Changes in chemical shift can potentially be used to monitor conformational changes, substrate binding, changes in the hydrogen-bonding and protonation state of the molecule studied. ^{17}O chemical shifts are referenced against H_2O .

Since the first application of ^{17}O solid-state NMR on MnO_2 by Jackson in 1963 [46], many other molecules have been characterized using this technique. The

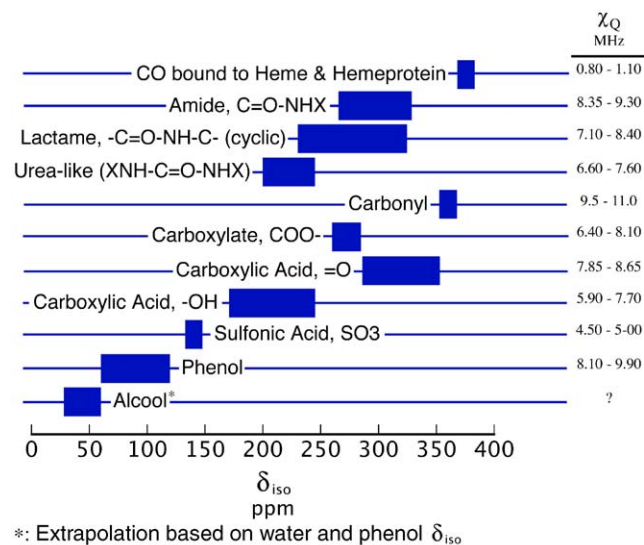


Fig. 5. ^{17}O isotropic chemical shift and quadrupole coupling constant ranges for different X–O bonds of organic molecules in the solid-state. There are some significant changes between solution (see [19]) and solid-state.

general trend of ^{17}O chemical shifts is shown in Fig. 5, which is the result of the compilation of about 30 reports from the last 20 years or so. This figure is not exhaustive, since the number of organic molecules that have been studied by ^{17}O solid-state NMR remains small and thus the examples given may not be representative of the entire chemical shift range of ^{17}O . The identity of the molecules and the individual values for the isotropic chemical shift (and also other parameters) can be found in Table 2. An important point to emphasize here is that the shift of the peak position in a solid state NMR spectrum of a second-order quadrupolar perturbed system does not correspond to the isotropic chemical shift (which is usually the case for solution spectra). If a second-order quadrupolar lineshape can be resolved then the isotropic chemical shift can be deduced from a single spectrum. Alternatively the field variation of the DOR peak position, or the centres of gravity in the two dimensions of an MQMAS NMR spectrum at a single field can be used. Care has to be taken to ascertain if papers when referring to the chemical shift, mean the peak position or the genuine isotropic value. In examining differences (e.g. from structural effects) it is isotropic chemical shifts that should be compared.

The values of the ^{17}O NMR chemical shifts for organic molecules in the solid-state measured to date cover a range from 46 to 375 ppm. Comparison with similar chemical shift ranges measured in solution [47] shows significant differences, up to 100 ppm. This is mainly due to important modifications in the hydrogen-bond network experienced by the different chemical groups upon crystallization. Most of the changes tend to

reduce the chemical shift of a specific chemical group from solution to solid-state and can be interpreted as an increase of the hydrogen-bond length (vide infra). The correlation between the C–O π bond order [48], observed in solution is also seen in the solid state. Another feature mirroring that in solution, is the small chemical shift range observed for S–O bonds, which cannot be related to the bond order in a similar manner as for C–O bonds.

5.2. Quadrupole coupling constant

Solid-state NMR allows the determination of parameters like χ_Q and η_Q (Table 2) from powder or single-crystal static experiments, and MAS of polycrystalline samples. However, it is not the only method available to provide information on quadrupole interaction related parameters. A significant number of quadrupole coupling constants of organic molecules have been determined using nuclear quadrupole resonance (NQR) spectroscopy [19,49–55] (see Table 3).

Solid-state NMR has shown that experimental χ_Q values cover the range 4.8–10.8 MHz for organic molecules in the solid-state, while nuclear quadrupole resonance (NQR) suggests values for the components of the quadrupole tensor from –9 to +11.5 MHz for chemical groups involving C–O bonds [55]. The sign of χ_Q gives information on the orientation of the field gradient. Fig. 5 summarizes values for quadrupolar coupling constants that have been measured for different chemical functions of crystalline organic molecules. Similarly to the isotropic chemical shifts, significant differences for χ_Q have been observed between the solution and solid-state [45,56]. The range over which χ_Q is distributed seems to be narrower in the solid-state compared to solution (–8–17 MHz) [19], again highlighting some effects of the hydrogen-bond network.

The general rule observed for the solution state [19], that a decrease of the quadrupole coupling constant occurs with an increase of strength of hydrogen bonding, is also a general trend observed in the solid-state (vide infra).

5.3. Ab initio calculations

The detailed quantum chemical description of sites in organic molecules is rather complex. The most common approach to simplify the modelling of the nuclear spin interactions is to consider them independently from the rest of the system, using lattice relaxation terms. Other considerations can be used to simplify the modelling process of ^{17}O chemical shift and other relevant parameters. Reports of calculations of the ^{17}O NMR parameters in such materials have been presented to varying degrees of sophistication, including Finite

Perturbation theory, Hartree–Fock and Density Functional Theory.

It is often found that inclusion of the hydrogen-bond network is necessary to achieve a good quality of fit, emphasizing how sensitive ^{17}O is regarding this type of interaction.

Wu et al. [57] used CP MAS to determine the amplitude and orientation of tensor interactions. They carried out DFT calculations with and without inclusion of an intermolecular hydrogen-bond network. Simulations using the software Gaussian (G98) with B3LYP as a level of theory, G-311+FG as a basis set and exchange functions Gauge including atomic orbital (GIAO) basis, have been performed for calculating the CS shielding.

There has been significant recent progress in first principles quantum mechanical calculation of NMR parameters that have greatly improved in theory, accuracy and speed with which they can be carried out. Rather than cluster-based calculations density functional theory using the Gauge including projector augmented wave (GIPAW) method [58] uses the true periodic nature of the crystal structure. The crystal structure is refined, by allowing the positions of the hydrogen atoms to relax. In the method, pseudopotentials are used to represent the electron cores. From these calculations both the chemical shielding and quadrupole interactions can be determined. Calculations of these parameters for ^{17}O using this approach have been applied to zeolites [59] and glutamic acid polymorphs [60]. For L-glutamic acid the quality of the calculations meant that the peaks could confidently be assigned on the basis of these calculations and illustrates the complementarity between the solid state NMR measurements and the computational work. Computational work will also allow correlations with structural detail to be explored without having to prepare as many enriched samples. Calculations can also help determine the orientation of the chemical shift and quadrupole interactions relative to one another. In powder samples combining variable magnetic field, and static and MAS data allows both the interactions and their orientation to be estimated, especially if ^1H decoupling is used to remove dipolar interactions. It is however difficult from this data alone to deduce the orientation of these interactions relative to the molecular frame, whereas single crystal measurements can provide this information.

5.4. Assignment of ^{17}O NMR resonances

In most ^{17}O NMR studies of organic molecules to date the assignment of the different resonances has been relatively straightforward, with the number of different sites small—two different signals on average. Furthermore, the crystal structure of the molecule under study is

almost always known. For this type of sample, an assignment based on the measurement of the chemical shift from a MAS experiment is usually sufficient, provided the two atoms belong to different chemical functions. As an example, for a molecule containing a single carboxylic group, the difference in NMR parameters between the hydroxyl ($-\text{OH}$, 170–190 ppm, $\chi_Q=8.6\text{--}8.0\text{ MHz}$) and the carbonyl ($=\text{O}$, 300–355 ppm, $\chi_Q=7.7\text{--}7.35\text{ MHz}$) is usually large enough to avoid any assignment confusion [45]. In amino acid·HCl materials the two resonances are completely resolved and the carbonyl and hydroxyl can be immediately identified. However in L-alanine, where there is a carboxylate group in a zwitterionic form, there is complete overlap between the two resonances as the isotropic chemical shifts differ by only 24 ppm so that it is difficult to directly uniquely identify the resonances.

To help assignment of the oxygen sites approaches using the strength of the coupling between the oxygen and surrounding protons have been applied. Typically, to understand the strength of the $^1\text{H}\text{--}^{17}\text{O}$ dipolar coupling, MAS or DOR experiments can be run where the strength of the proton decoupling is varied [45]. The DOR experiment allows the best resolution of the different signals (line widths down to 1 ppm [45]). Then, the line broadening as a function of the decoupling strength allows the assignment of a specific site from the crystal structure. The narrower the line, the less strongly is a particular oxygen atom coupled to the protons.

MQMAS can also be used for helping the attribution of signals to particular sites within the crystal structure [34]. From MQMAS data it has been shown that the isotropic chemical shift increases with a decrease in hydrogen-bond length (based on the carbonyl bond length that increases if the strength of the hydrogen-bond increases).

Another technique used previously in solid-state ^{17}O NMR studies was to record spectra at different temperatures: the oxygen involved in the weakest hydrogen-bond network show the most significant changes in its NMR parameters. The method was demonstrated with L-leucine where two types of hydrogen-bonding in the unit cell can be distinguished [61].

All the methods developed so far are limited, in the sense they only allow a small number of different oxygen sites to be dealt with and their chemical environment should ideally differ significantly to allow ready assignment. Furthermore, X-ray or neutron diffraction structures are required in order to determine how each oxygen atom is involved in the hydrogen-bond network. Future work will have to include development of self-consistent NMR methods in order to assign ^{17}O signals in an independent way without relying on previously available structural information, and the computational work mentioned above will play an important role here.

Table 2
 ^{17}O NMR parameters of organic molecules in the solid-state

		$\delta_{\text{cs,iso}}$ (ppm)	χ_Q (MHz)	η_Q	σ_{11} (ppm)	σ_{22} (ppm)	σ_{33} (ppm)	α (deg)	β (deg)	γ (deg)	Ref.	Structure ref.
<i>Organic molecules</i>												
Benzophenone	O	358 ± 42	10.808	0.369	537 ± 42	525 ± 42	12 ± 42	—	—	—	[66]	[67]
Benzamide	O	300	8.40	0.40	500 ± 3	400 ± 3	0 ± 3	—	—	—	[23]	[68]
Benzanilide	O	320	8.97	0.15	580 ± 5	450 ± 5	-50 ± 5	5	90	70	[23,62]	[69]
<i>N</i> -Methylbenzamide	O	287	8.50	0.30	520	380	-40	5	90	78	[62]	[70]
Acetanilide	O	330	8.81	0.20	570	440	-20	0	89	69	[62]	[71]
2-Nitro- ^{17}O -phenol	OH	63	9.90	0.8	—	—	—	—	—	—	[23]	[72]
4-Nitro- ^{17}O -phenol	OH	80	9.70	0.85	—	—	—	—	—	—	[23]	[73]
DL-Tyrosine · HCl	OH	117	8.10	1.0	—	—	—	—	—	—	[23]	[74]
α -Oxalic Acid	O1 (C=O)	301 ± 14	8.30 ± 0.23	0.07	476 ± 18	413 ± 11	14 ± 13	22 ± 12	26 ± 12	20 ± 1	[75]	[76]
	O2 (C-OH)	183 ± 4	6.68 ± 0.08	0.16	351 ± 4	142 ± 3	55 ± 4	10 ± 1	5 ± 3	9 ± 1		
Benzoic acid	O	230	5.70	1.0	—	—	—	—	—	—	[23]	[77]
Potassium hydrogen benzoate	O1 (C=O)	290	8.50	0.20	—	—	—	—	—	—	[23]	[78]
	O2 (C-OH)	230	6.30	0.10	—	—	—	—	—	—		
Potassium hydrogen benzoate	O1 (C=O)	287 ± 2	8.30 ± 0.02	0.23 ± 0.05	470 ± 5	380 ± 5	10 ± 5	0 ± 5	90 ± 5	30 ± 5	[79]	[78]
	O2 (C-OH)	213 ± 2	5.90 ± 0.02	0.55 ± 0.05	370 ± 5	190 ± 5	80 ± 5	5 ± 5	90 ± 5	90 ± 5		
Potassium hydrogen benzoate	O1 (C=O)	285 ± 5	8.30	0.15 ± 0.01	—	—	—	—	—	—	[80]	[78]
	O2 (C-OH)	215 ± 5	5.90 ± 0.02	0.90 ± 0.01	—	—	—	—	—	—		
Ammonium hydrogen benzoate	O1 (C-OH)	240	6.3	0.40	—	—	—	—	—	—	[23]	[81]
	O2 (C-OHN)	242	6.3	0.0	—	—	—	—	—	—		
Phthalic Acid	O1 (C=O)	312 ± 5	7.2 ± 0.1	0 ± 0.05	—	—	—	—	—	—	[82]	[83]
	O2 (C-OH)	180 ± 5	7.4 ± 0.1	0 ± 0.05	—	—	—	—	—	—		
Lithium hydrogen phthalate · 2 H ₂ O	O	46 ± 5	5.9 ± 0.1	0.21 ± 0.05	—	—	—	—	—	—	[82]	[84]
Dilithium phthalate hemihydrate	O	272 ± 5	7.6 ± 0.1	0.44 ± 0.05	—	—	—	—	—	—	[82]	NA
Potassium hydrogen phthalate · 2 H ₂ O	O	305 ± 5	8.4 ± 0.1	0.20 ± 0.05	—	—	—	—	—	—	[82]	[85]
<i>p</i> -Toluenesulfonic acid · H ₂ O	O (S-O)	140	4.79	1.0	—	—	—	—	—	—	[23]	[86]
Urea	O	200 ± 1	7.24 ± 0.01	0.92	—	—	—	0	90	0/90	[56]	[87,88]

Nucleic acid bases

2- ¹⁷ O-Cytosine	O2	230	7.20	0.70	350	300	40	12	80	70	[63]	[89,90]
6- ¹⁷ O-Guanine · H ₂ O	O6	230	7.10	0.80	395	285	10	5	87	67	[63]	[91]
2- ¹⁷ O-Thymine	O2	200 ± 2	6.65 ± 0.02	1.00 ± 0.02	290 ± 5	270 ± 5	20 ± 5	4	90	70	[63,64]	[92]
4- ¹⁷ O-Thymine	O4	325 ± 2	8.40 ± 0.02	0.10 ± 0.02	570 ± 5	360 ± 5	20 ± 5	0	84	84	[63,64]	[92]
[2-4- ¹⁷ O ₂]Uracil	O2	240 ± 5	7.62 ± 0.02	0.50 ± 0.01	—	—	—	—	—	—	[34]	[93]
	O4	275 ± 5	7.85 ± 0.02	0.55 ± 0.01	—	—	—	—	—	—	—	—
2- ¹⁷ O-Uracil	O2	245	7.61	0.50	400	330	10	0	89	82	[63]	[93]
4- ¹⁷ O-Uracil	O4	275	7.85	0.55	470	350	10	0	90	75	[63]	[93]

Amino acids

L-Alanine	O	—	6.6	0.55	50	350	350	—	—	—	[24]	[94]
L-Alanine	O1	285 ± 8	8.1 ± 0.3	—	—	—	—	—	—	—	[95]	[94]
	O2	268 ± 8	7.2 ± 0.3	—	—	—	—	—	—	—	—	—
L-Alanine	O1	284 ± 0.5	7.86 ± 0.05	0.28 ± 0.02	—	—	—	—	—	—	[45]	[94]
	O2	260.5 ± 0.5	6.53 ± 0.05	0.70 ± 0.02	—	—	—	—	—	—	—	—
L-Alanine · HCl	O1	327.8 ± 0.5	8.31 ± 0.05	0.00 ± 0.02	—	—	—	—	—	—	[45]	[96]
	O2	176.7 ± 0.5	7.29 ± 0.05	0.20 ± 0.02	—	—	—	—	—	—	—	—
Fmoc-L-Alanine	O1	303.3 ± 0.5	7.89 ± 0.05	0.16 ± 0.02	—	—	—	—	—	—	[45]	NA
	O2	175.7 ± 0.5	6.95 ± 0.05	0.12 ± 0.02	—	—	—	—	—	—	—	—
D-Alanine	O1	275 ± 5	7.60 ± 0.02	0.60 ± 0.01	—	—	—	—	—	—	[34]	NA See [94]
	O2	262 ± 5	6.40 ± 0.02	0.65 ± 0.01	—	—	—	—	—	—	—	—
L-Cysteine · HCl	O1	353.5 ± 0.5	8.65 ± 0.05	0.18 ± 0.02	—	—	—	—	—	—	[45]	NA
	O2	174.9 ± 0.5	7.41 ± 0.05	0.27 ± 0.02	—	—	—	—	—	—	—	—
L-Glutamic acid · HCl	O1 or O4	172.5 ± 0.5	7.45 ± 0.05	0.25 ± 0.02	—	—	—	—	—	—	[35]	[97]
	O1 or O4	187.0 ± 0.5	7.49 ± 0.05	0.25 ± 0.02	—	—	—	—	—	—	—	—
	O2	322.0 ± 0.5	8.16 ± 0.05	0.00 ± 0.03	—	—	—	—	—	—	—	—
	O3	315.0 ± 0.5	8.31 ± 0.05	0.17 ± 0.02	—	—	—	—	—	—	—	—
D-Glutamic acid · HCl	O1 or O4	172.3 ± 0.5	7.45 ± 0.05	0.25 ± 0.02	—	—	—	—	—	—	[45]	NA See [97]
	O1 or O4	187.2 ± 0.5	7.49 ± 0.05	0.25 ± 0.02	—	—	—	—	—	—	—	—
	O3	315.4 ± 0.5	8.16 ± 0.05	0.00 ± 0.03	—	—	—	—	—	—	—	—
	O2	322.0 ± 0.5	8.31 ± 0.05	0.17 ± 0.02	—	—	—	—	—	—	—	—
DL-Glutamic acid · HCl	O1	170 ± 5	7.20 ± 0.02	0.20 ± 0.01	—	—	—	—	—	—	[34]	NA
	O2 & O3	250 ± 5	6.80 ± 0.02	0.58 ± 0.01	—	—	—	—	—	—	—	—
	O4	320 ± 5	8.20 ± 0.02	0.00 ± 0.01	—	—	—	—	—	—	—	—
Monosodium L-Glutamate · H ₂ O	1	254 ± 1.5	7.4 ± 0.2	0.47 ± 0.05	—	—	—	—	—	—	[35]	[98]
	2	260 ± 1.5	7.2 ± 0.2	0.50 ± 0.05	—	—	—	—	—	—	—	—
	3	274 ± 1.5	7.6 ± 0.2	0.45 ± 0.05	—	—	—	—	—	—	—	—
	4	283 ± 1.5	7.7 ± 0.2	0.40 ± 0.05	—	—	—	—	—	—	—	—
	5	297 ± 1.5	7.0 ± 0.2	0.45 ± 0.05	—	—	—	—	—	—	—	—
L-Glutamine · HCl	O1	319.8 ± 0.5	8.20 ± 0.05	0.03 ± 0.02	—	—	—	—	—	—	[45]	[99]
	O2	306 ± 1	8.30 ± 0.1	0.03 ± 0.03	—	—	—	—	—	—	—	—
	O3	180 ± 1	7.75 ± 0.05	0.24 ± 0.02	—	—	—	—	—	—	—	—
Glycine · HCl	O1	336 ± 0.5	8.40 ± 0.05	0.00 ± 0.02	—	—	—	—	—	—	[45]	[96]
	O2	185 ± 0.5	7.60 ± 0.05	0.25 ± 0.02	—	—	—	—	—	—	—	—
L-Isoleucine · HCl	O1	347.1 ± 0.5	8.52 ± 0.05	0.06 ± 0.02	—	—	—	—	—	—	[45]	NA
	O2	182.6 ± 0.5	7.40 ± 0.05	0.22 ± 0.02	—	—	—	—	—	—	—	—
Leucine · HCl	O1	342.7 ± 0.5	8.39 ± 0.05	0.05 ± 0.02	—	—	—	—	—	—	[45]	NA
	O2	182.6 ± 0.5	7.50 ± 0.05	0.20 ± 0.02	—	—	—	—	—	—	—	—
L-Lysine · HCl	O1	346.7 ± 0.5	8.56 ± 0.05	0.00 ± 0.02	—	—	—	—	—	—	[45]	NA

Table 2 (continued)

		$\delta_{\text{cs,iso}}$ (ppm)	χ_Q (MHz)	η_Q	σ_{11} (ppm)	σ_{22} (ppm)	σ_{33} (ppm)	α (deg)	β (deg)	γ (deg)	Ref.	Structure ref.
L-Phenylalanine · HCl	O2	180.8 ± 0.5	7.67 ± 0.05	0.24 ± 0.02	—	—	—	—	—	—	[45]	[100]
	O1	353.5 ± 0.5	8.54 ± 0.05	0.07 ± 0.02	—	—	—	—	—	—		
	O2	178.8 ± 0.5	7.46 ± 0.05	0.25 ± 0.02	—	—	—	—	—	—		
L-Tyrosine · HCl	O1	327.0 ± 0.5	8.22 ± 0.05	0.00 ± 0.02	—	—	—	—	—	—	[45]	[101]
	O2	183.0 ± 0.5	7.35 ± 0.05	0.19 ± 0.02	—	—	—	—	—	—		
	O3	83.0 ± 0.5	8.56 ± 0.05	0.65 ± 0.02	—	—	—	—	—	—		
	O3	117 ± 0.5	8.10 ± 0.05	1.0 ± 0.02	—	—	—	—	—	—		
D,L-Tyrosine · HCl	O1	351 ± 0.5	8.40 ± 0.05	0.03 ± 0.02	—	—	—	—	—	—	[23]	NA
L-Valine · HCl	O1	351 ± 0.5	8.40 ± 0.05	0.03 ± 0.02	—	—	—	—	—	—	[45]	[102]
	O2	181 ± 0.5	7.35 ± 0.05	0.21 ± 0.02	—	—	—	—	—	—		
Fmoc-L-valine	O1	324.1 ± 0.5	8.42 ± 0.05	0.08 ± 0.02	—	—	—	—	—	—	[45]	NA
	O2	167.3 ± 0.5	7.48 ± 0.05	0.27 ± 0.02	—	—	—	—	—	—		
<i>Peptides/polypeptides</i>												
GlyGly	O	265	8.55	0.45	546	382	−132	94	90	−87	[39]	[103]
GlyGly · HNO ₃	O	280	8.75	0.47	559	408	−127	94	89	−81	[39]	[104]
Polyglycine I (3 ₁₀ -helix)	O	299	8.55	0.26	574	425	−101	100	91	−79	[39]	[105]
Polyglycine I(3 ₁₀ -helix) (3 ₁₀ -helix)	O	304	8.36	0.30	—	—	—	—	—	—	[14]	[105]
Polyglycine II (β-sheet)	O	299	8.30	0.29	562	410	−108	92	89	−81	[39]	[106,107]
Polyglycine II (β-sheet)	O	293	8.21	0.33	—	—	—	—	—	—	[14]	[106,107]
Poly(L-alanine) (α-helix)	O	303	9.28	0.33	595	435	−121	—	—	—	[65]	[108]
Poly(L-alanine) (α-helix)	O	319	8.59	0.28	—	—	—	—	—	—	[13]	[108]
Poly(L-alanine) (β-sheet)	O	265	8.65	0.41	514	390	−110	—	—	—	[65]	[109]
Poly(L-alanine) (β-sheet)	O	286	8.04	0.28	—	—	—	—	—	—	[13]	[109]
<i>Inorganic molecules complexed with organic molecules or proteins</i>												
p-Toluenesulfonic acid · H ₂ O	O (H ₂ O)	30.0 ± 0.5	7.05 ± 0.02	0.0	88 ± 2	1 ± 2	1 ± 2	—	—	—	[110]	[86]
Oxalic acid dihydrate	O (H ₂ O)	—	6.80 ± 0.20	0.93 ± 0.10	—	—	—	—	—	—	[111]	[112]
C ¹⁷ O bound to Fe(TPP)(CO)(NmeIm)	O (CO)	372	1.0	—	—	—	—	—	—	—	[113]	—
C ¹⁷ O bound to A ₀ Myoglobin	O (CO)	372	1.1	—	—	—	—	—	—	—	[113]	—
C ¹⁷ O bound to A ₁ Myoglobin	O (CO)	366	0.8	—	—	—	—	—	—	—	[113]	—

Note: Usually, ¹⁷O solid-state NMR spectra are referenced relative to natural abundance water at room temperature, for which the chemical shift is arbitrarily set to 0 ppm. This gives a sharp resonance and there is a very small shift dependence on pH but this is not normally taken into account.

Table 3
¹⁷O quadrupole parameters of selected organic molecules in the solid-state determined by NQR double resonance studies

		χ_Q (MHz)	η_Q	Ref.
<i>Organic molecules</i>				
Acetic acid (220 K)	O1 (C=O)	$\pm 8.108 \pm 0.005$	0.15 ± 0.01	[50]
	O2 (C–OH)	-7.280 ± 0.005	0.187 ± 0.005	
Acrylic acid (77 K)	O1 (C=O)	$\pm 7.565 \pm 0.005$	0.31 ± 0.01	[50]
	O2 (C–OH)	-7.195 ± 0.005	0.166 ± 0.005	
Aspirin (291 K)	O1 (C=O)	6.793 ± 0.005	0.551 ± 0.005	[51]
	O2 (C–OH)	-6.683 ± 0.005	0.224 ± 0.005	
Benzoic acid (291 K)	O1 (C=O)	5.780 ± 0.007	0.894 ± 0.007	[51]
	O2 (C–OH)	-5.917 ± 0.005	0.736 ± 0.005	
α -Chloroacetic acid (77 K)	O1 (C=O)	$\pm 8.207 \pm 0.010$	0.157 ± 0.01	[50]
	O2 (C–OH)	-7.494 ± 0.005	0.216 ± 0.007	
<i>p</i> -Chloro-benzoic acid (291 K)	O1 (C=O)	6.113 ± 0.007	0.769 ± 0.008	[51]
	O2 (C–OH)	-6.409 ± 0.005	0.387 ± 0.005	
<i>m</i> -Chloro-benzoic acid (291 K)	O1 (C=O)	6.440 ± 0.020	0.565 ± 0.012	[51]
	O2 (C–OH)	-6.610 ± 0.020	0.250 ± 0.015	
Cyanoacetic acid (77 K)	O1 (C=O)	$\pm 8.093 \pm 0.015$	0.028 ± 0.01	[50]
	O2 (C–OH)	-7.427 ± 0.005	0.083 ± 0.005	
Formic acid (77 K)	O1 (C=O)	$\pm 7.818 \pm 0.005$	0.07 ± 0.02	[50]
	O2 (C–OH)	-0.900 ± 0.005	0.077 ± 0.005	
Fumaric acid (77 K)	O1 (C=O)	$\pm 8.226 \pm 0.010$	0.125 ± 0.025	[50]
	O2 (C–OH)	-7.400 ± 0.010	0.185 ± 0.010	
Hydroxyacetic acid (77 K)	O1 (C=O)	$\pm 8.068 \pm 0.015$	0.106 ± 0.01	[50]
	O2 (C–OH)	-7.304 ± 0.010	0.236 ± 0.010	
<i>p</i> -Hydroxy-benzoic acid (291 K)	O1 (C=O)	5.873 ± 0.007	0.820 ± 0.008	[51]
	O2 (C–OH)	-5.945 ± 0.007	0.730 ± 0.007	
<i>m</i> -Hydroxy-benzoic acid (291 K)	O1 (C=O)	5.756 ± 0.008	0.812 ± 0.005	[51]
	O2 (C–OH)	-5.996 ± 0.008	0.660 ± 0.007	
Imidazolium hydrogen maleate (291 K)	O (O–H–O)	6.105 ± 0.015	0.620 ± 0.010	[52]
Isophthalic acid (291 K)	O1 (C=O)	7.198 ± 0.010	0.416 ± 0.010	[51]
	O2 (C–OH)	-6.765 ± 0.010	0.155 ± 0.010	
Maleic acid (77 K)	O1 (C=O)	$\pm 7.485 \pm 0.010$	0.28 ± 0.01	[50]
	O2 (C=O)	$\pm 8.593 \pm 0.010$	0.105 ± 0.015	
	O3 (C–OH)	-7.000 ± 0.020	0.04 ± 0.03	
	O4 (C–OH)	-7.233 ± 0.010	0.04 ± 0.02	
Maleic acid (295 K)	O1 (C=O)	$\pm 7.480 \pm 0.010$	0.28 ± 0.01	[50]
	O2 (C=O)	$\pm 8.545 \pm 0.010$	0.085 ± 0.02	
	O3 (C–OH)	-6.935 ± 0.010	0.05 ± 0.02	
	O4 (C–OH)	-7.175 ± 0.010	0.085 ± 0.015	
<i>p</i> -Nitro-benzoic acid (291 K)	O1 (C=O)	5.985 ± 0.005	0.850 ± 0.008	[51]
	O2 (C–OH)	-6.166 ± 0.007	0.519 ± 0.007	
<i>m</i> -Nitro-benzoic acid (291 K)	O1 (C=O)	5.950 ± 0.017	0.790 ± 0.015	[51]
	O2 (C–OH)	-6.385 ± 0.010	0.360 ± 0.008	
<i>o</i> -Nitro-benzoic acid (291 K)	O1 (C–OH)	-5.461 ± 0.020	0.770 ± 0.015	[51]
	O2 (C–OH)	-6.046 ± 0.020	0.450 ± 0.010	
α -Oxalic acid (77 K)	O1 (C=O)	$\pm 8.455 \pm 0.003$	0.00 ± 0.01	[50]
	O2 (C–OH)	-7.545 ± 0.010	0.160 ± 0.010	
α -Oxalic acid (295 K)	O1 (C=O)	$\pm 8.471 \pm 0.003$	0.00 ± 0.01	[50]
β -Oxalic acid (77 K)	O1 (C=O)	$\pm 8.110 \pm 0.007$	0.08 ± 0.02	[50]
	O2 (C–OH)	-7.350 ± 0.010	0.135 ± 0.010	
β -Oxalic acid (291 K)	O1 (C=O)	$\pm 7.473 \pm 0.008$	0.237 ± 0.005	[51]
	O2 (C–OH)	-6.933 ± 0.008	0.000 ± 0.020	
β -Oxalic acid (295 K)	O1 (C=O)	$\pm 7.473 \pm 0.010$	0.24 ± 0.01	[50]
	O2 (C–OH)	-6.930 ± 0.010	0.00 ± 0.02	
Phthalic acid (291 K)	O1 (C=O)	7.078 ± 0.007	0.405 ± 0.008	[51]
	O2 (C–OH)	-7.173 ± 0.005	0.147 ± 0.005	
Potassium hydrogen benzoate (291 K)	O (O–H–O)	6.165 ± 0.007	0.591 ± 0.007	[52]
Potassium hydrogen chloromaleate (291 K)	O (O–H–O)	6.330 ± 0.010	0.580 ± 0.020	[52]
Potassium hydrogen diaspirinate (291 K)	O (O–H–O)	6.214 ± 0.015	0.551 ± 0.015	[52]
Potassium hydrogen di- <i>m</i> -chlorobenzoate (291 K)	O (O–H–O)	6.248 ± 0.010	0.599 ± 0.008	[52]
Potassium hydrogen di- <i>p</i> -chlorobenzoate (291 K)	O (O–H–O)	6.213 ± 0.008	0.569 ± 0.007	[52]
Potassium hydrogen diformate (291 K)	O1 (C=O)	5.462 ± 0.008	0.833 ± 0.008	[52]
	O2 (C–OH)	5.641 ± 0.008	0.539 ± 0.007	
Potassium hydrogen maleate (291 K)	O (O–H–O)	6.074 ± 0.010	0.589 ± 0.020	[52]

Table 3 (continued)

		χ_Q (MHz)	η_Q	Ref.
Potassium hydrogen oxalate (291 K)	O1 (C=O)	6.637 ± 0.015	0.684 ± 0.010	[52]
	O2 (C–OH)	6.911 ± 0.010	0.086 ± 0.010	
Potassium hydrogen phthalate (291 K)	O1 (C=O)	6.611 ± 0.015	0.758 ± 0.010	[52]
	O2 (C–OH)	7.133 ± 0.010	0.000 ± 0.010	
Quinolic acid (291 K)	O1 (C=O)	6.126 ± 0.015	0.745 ± 0.010	[52]
	O2 (C–OH)	6.277 ± 0.015	0.633 ± 0.010	
Salicylic acid (291 K)	O1 (C=O)	-5.319 ± 0.008	0.860 ± 0.008	[51]
	O2 (C–OH)	-5.825 ± 0.008	0.624 ± 0.007	
	O3 (C–OH)	9.197 ± 0.020	0.982 ± 0.010	
<i>Amino acid</i>				
DL-Proline	A1	6.79	0.170	
	A2	6.45	0.436	
	A3	6.17	0.663	
	A4	6.08	0.703	
	B1	7.72	0.242	
	B2	7.78	0.150	
	B3	8.28	<0.1	
	B4	8.37	<0.05	

6. Selected applications

6.1. Organic molecules, nucleic acid and amino acids

Recent reports of ^{17}O NMR from organic materials have included hemeproteins, polypeptides, strongly hydrogen-bonded carboxylic acids, amino acids and nucleic acid bases.

Several classes of molecules have been more extensively studied, amongst them the individual components of DNA and proteins, including the nucleic acids (all of them) and a vast majority of the naturally occurring amino acids. It has to be noted that carbohydrates, an important class of biologically important molecules with high oxygen content, have not been studied yet. The alcohol group is another chemical functionality that has not yet received much attention, with no solid-state NMR report to date. The closest study to this functionality is that of a few phenolic molecules (2-nitrophenol, 4-nitrophenol and tyrosine) [23], characterized by wider signals than for amide groups.

The amide group has been investigated as a simplified model for the amide bond that mediates the link between the different amino acid residues, and is also present in several nucleic acid bases (T, G and U). Wu et al. explored several of them (benzanilide, *N*-methyl benzamide, acetanilide) [57,62], determining the chemical shift tensor orientation.

Nucleic acid bases have been studied [34,63,64] (Fig. 6). Uracil had both one (static and MAS) [63,64] and two oxygen sites labelled (MAS and MQMAS) [34]. From this work all the components of the EFG and CS tensor have been determined for all the nucleobases (amplitude and relative orientation). Furthermore, it has allowed comparison with the same molecules in

solution, showing that for some oxygen sites, there are very large changes upon crystallization. The nature of those changes is related with the degree of involvement of each particular oxygen atom in the intermolecular hydrogen-bond network. The oxygen atoms that are able to form intramolecular hydrogen bonds show smaller changes in their NMR parameters upon crystallization. ^{17}O MAS gives line widths up to 10 kHz highlighting the sizable residual quadrupolar width. Static spectra show line widths from 30 to 60 kHz. Accuracy of the simulation is estimated to ± 10 ppm for chemical shift and $\pm 5^\circ$ for Euler angles [63,64].

Amino acids were amongst the first organic molecules to be studied by ^{17}O solid-state NMR, beginning as early as 1988 [24,61]. At this time, the resolution was low and it took about 5 h with a Bruker CXP 180 to collect a spectrum with a *S/N* of 20 for a sample with an enrichment of 20 at% in ^{17}O . In the case of the L-leucine where there are two inequivalent molecules per unit cell, only two inequivalent sites could be found. It was not possible to resolve the two oxygen sites of L-alanine before 1994 and the application of DAS. The EFG and CS tensors in the molecular frame could nevertheless be estimated in the earlier work [24].

All the ^{17}O solid-state NMR techniques available have now been applied to amino acids namely, static NMR on powders and single crystals as well as polycrystals, MAS, DAS, DOR and 3QMAS on polycrystalline materials.

Application of higher resolution techniques have highlighted how sensitive the ^{17}O NMR parameters of labelled amino acids are relative to crystallization conditions (pH) [35,45] or even modification of the amino-group of the molecules [45] (e.g. Fmoc protection of the amino group). In those cases, major changes in

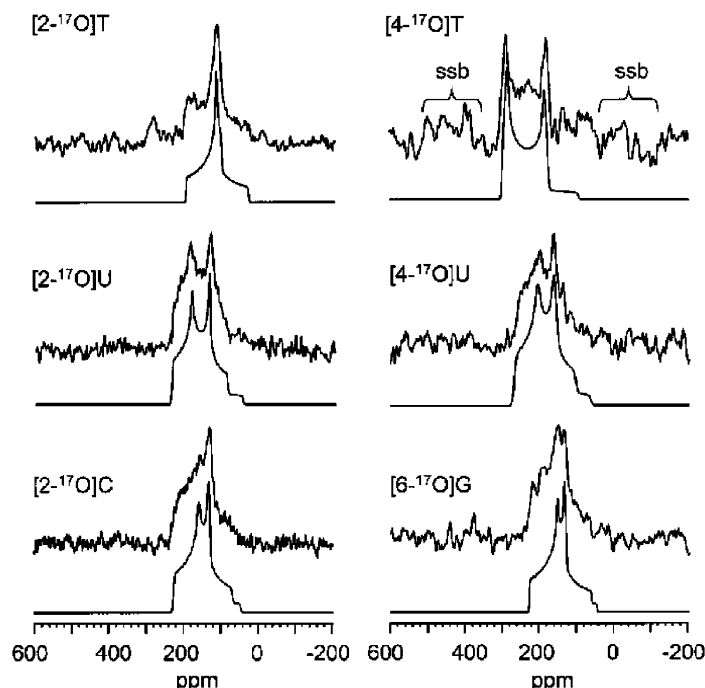


Fig. 6. Experimental (upper trace) and simulated (lower trace) ^{17}O MAS NMR spectra of free nucleic acid bases at 11.75 T. Chemical shifts are referenced to liquid H_2O (adapted from [63] with permission of the copyright owner).

the shape and the frequencies of the signals have been observed (Fig. 7).

6.2. Small peptides and polymers

^{17}O solid-state NMR has been applied to study small peptides (glycylglycine and glycylglycine $\cdot \text{HNO}_3$ [39,40]) and uniformly labelled polypeptides (polyglycine I and II [14,38–40], poly(L-alanine) I and II [13,65]). Unfortunately, the low enrichment of the samples (6–10 at% for the different samples) has led to the observation of numerous artefacts in the observed spectra, many of which were recorded at lower applied magnetic fields.

Kuroki et al. [39] manufactured samples with a low enrichment, and the spectra accumulated at lower applied magnetic fields (9.39 T, 400 MHz ^1H) resulted in the authors reaching an erroneous conclusion about the carbonyl ^{17}O NMR parameters, especially regarding the orientation of the chemical shift tensor in the molecular frame [62]. This was corrected in later papers where MAS at 25 kHz was applied (18.8 T, 800 MHz ^1H) and the quality of the data significantly improved [13,14].

One of the most interesting applications of ^{17}O solid-state NMR on polypeptides illustrates the ability of the technique to differentiate between parallel and antiparallel chains in the case of a 3_{10} -helix, whereas ^{13}C and ^{15}N solid-state NMR were unable to resolve any differences. Kuroki et al. reported that ^{17}O solid-state NMR could be used to detect two inequivalent signals in

polyglycine II, that would only be consistent with an antiparallel 3_{10} -helix and not a parallel 3_{10} -helix [38,39]. The two inequivalent oxygen sites were not observed in more recent publications by the same authors, where the same samples were studied at higher magnetic field and with higher MAS rate [13].

Nevertheless, it is possible to determine accurately the ^{17}O NMR parameters on labelled peptides, which constitute the most complex organic samples studied by ^{17}O solid-state NMR so far. Indeed, the polypeptides studied are characterized by different degrees of polymerization (leading to a heterogeneous system) and different secondary structures can be obtained. Polyglycine I and II form, respectively, helix 3_{10} - and β -sheet, while poly(L-alanine) I and II forms are α -helix and β -sheet, respectively.

There is no doubt that in future, more samples with this level of complexity will be studied more routinely by ^{17}O NMR. Small oligopeptides and selectively labelled peptides in both crystalline or non-crystalline phases with a high enough enrichment level constitute an attainable goal for ^{17}O solid-state NMR and important structural information could be extracted from such samples [13,14].

6.3. Carbonyl group: the ^{17}O chemical shift as a picometer ruler

One over-riding feature of NMR in structural studies is the sensitivity of chemical shift and dipolar coupling

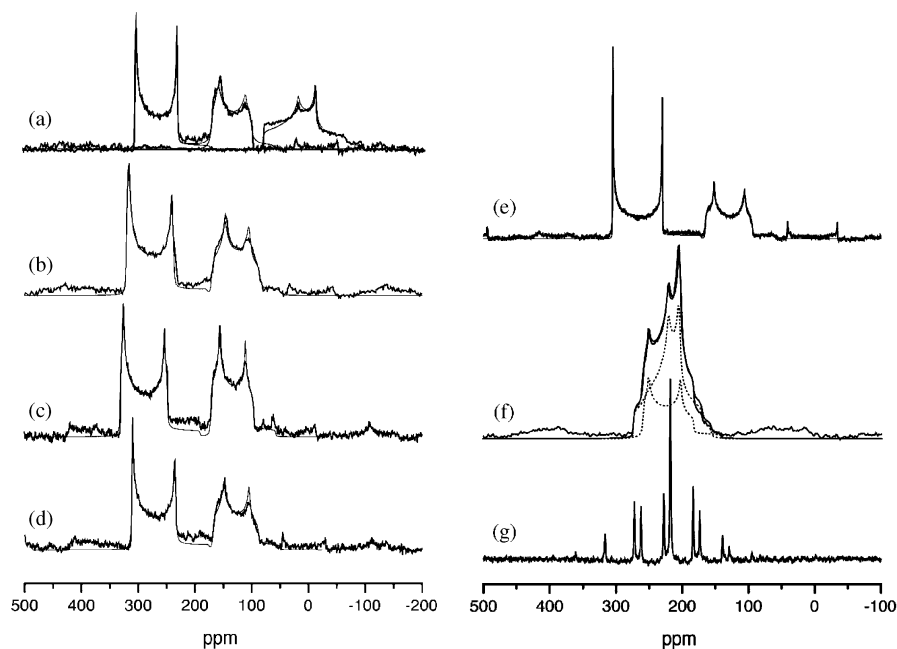


Fig. 7. 14.1 T ^{17}O MAS NMR spectra of (a) L-tyrosine·HCl, (b) L-asparagine·HCl, (c) L-valine·HCl, (d) glycine·HCl and (e) L-alanine·HCl together with simulations of the centrebands. (f) 14.1 T ^{17}O MAS NMR spectrum of L-alanine together with simulation, (g) DOR spectrum of L-alanine outer rotor speed 1800 Hz (adapted from [45]).

constants (D_{ab}) to internuclear distance ($r^3 \propto \frac{1}{D_{ab}}$). Thus for determination of local (over several hundreds of pm) distances, NMR surpasses virtually all other methods, both in accuracy and precision. For example, there is a good and strong ($\sim 1200 \text{ ppm}/\text{\AA}$) linear correlation of the chemical shift (δ_{iso}) of the carbonyl oxygen with the C–O bond length for ^{17}O labelled sites [45] (Fig. 8). The correlation is derived from the study of 9 amino acids co-crystallized with HCl and comparison of NMR δ_{iso} and the distance $R(\text{C}–\text{O})$ between the two atoms in the carbonyl moiety of the carboxylic acid group of those amino acids.

6.4. Study of hydrogen bonding

One of the core interests in applying ^{17}O solid-state NMR is to probe hydrogen bonding. Oxygen atoms are usually optimally located to monitor any hydrogen-bonds, and due to its quadrupolar nature, it should be very sensitive to any changes of the strength of such interactions. X-ray crystallographers have stated that the N–H \cdots O–C hydrogen bond is a universal feature of amino acid aggregation in the solid-state [114]. However, it has been now almost 10 years since several authors [39] have tried to correlate ^{17}O NMR parameters to molecular structure and hydrogen-bond length in particular.

So far, there is not a complete understanding between the hydrogen-bond properties (especially the bond-length) and the value of different NMR parameters.

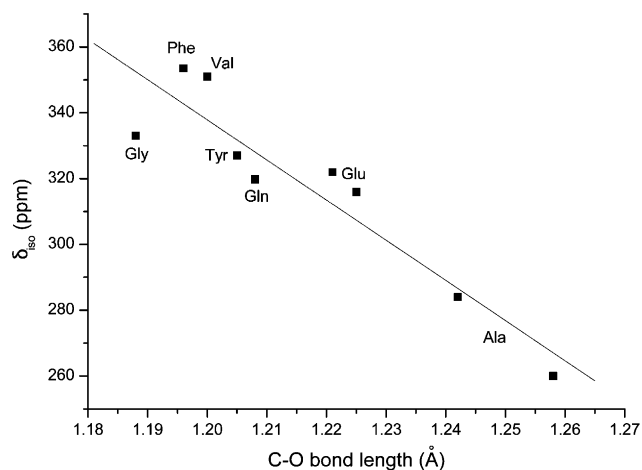


Fig. 8. Correlation between shift of the C=O oxygens with the C–O bond length (adapted from [45]).

General trends can be observed as well as limited correlations between bond-length and ^{17}O NMR parameters. This highlights the complexity of the hydrogen-bond interactions and the importance of the relative orientations between the different partners involved in the hydrogen bond.

In the case of N–H \cdots O=C hydrogen-bonds, it was shown that the quadrupole coupling tensor is a function of the $R(\text{N}\cdots\text{O})$ distance between the nitrogen and the oxygen, both theoretically [115] and experimentally [39,62]. However, a simple general correlation has not

yet been discerned. The following general trends have, nevertheless, been noted [13,14,39,56,62,63,65,115]:

1. e^2qQ/h decreases as the length of the hydrogen bond decreases (see Ref. [116] for a definition of hydrogen-bond length) (in other words, if the strength of the hydrogen bond increases);
2. The principal value σ_{33} of ^{17}O chemical shift tensor moves upfield if the length of the hydrogen bond decreases.

In summary, with an increase in hydrogen-bond strength, the shielding of the nucleus increases, so that both chemical shift and χ_Q decrease. Furthermore, it has been shown that virtually all ^{17}O NMR parameters vary upon changes in the local hydrogen bond network [62]. Wu and co-workers [56,57,63] have highlighted the importance of including the whole intermolecular hydrogen bond network in order to simulate accurately the components of the CS and EFG tensors.

Kuroki and co-workers have studied several dipeptides and polypeptides and tried to correlate e^2qQ/h with the $R(\text{N}\cdots\text{O})$ distance between the nitrogen and the oxygen (Fig. 9) [13,14,39]. According to simulations performed by Wu et al. [62] on the amide chemical function, σ_{11} and σ_{22} increase while σ_{33} decreases with the hydrogen bond length. The behaviour of the first two components of the CSA is in agreement with observation from Kuroki and co-workers [39], with the exception of some discrepancies for σ_{33} that might have resulted from a simulation artefact (a small basis set was used—STO-6G). In amides [62] asymmetry parameters (η_Q) decrease with hydrogen-bond length increasing hydrogen-bond length, while the quadrupole coupling constant increases (Fig. 10). As a result, χ_Q , η_Q , σ_{11} , σ_{22} and σ_{33} vary with the hydrogen bond-length in systems comprised of very similar molecules crystallizing in slightly different ways [62].

Hydrogen bonding for carbonyl groups often results in large upfield ^{17}O chemical shifts [39]. Furthermore, it seems the whole network of the hydrogen bonds and the

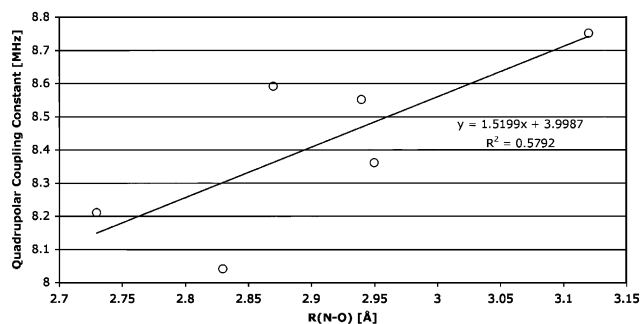
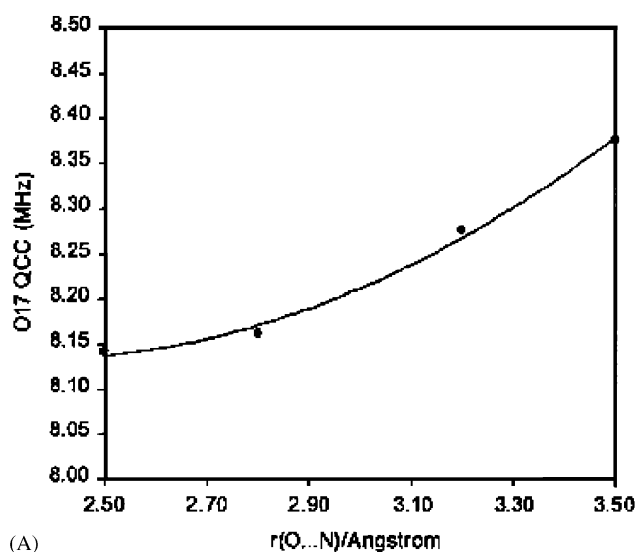


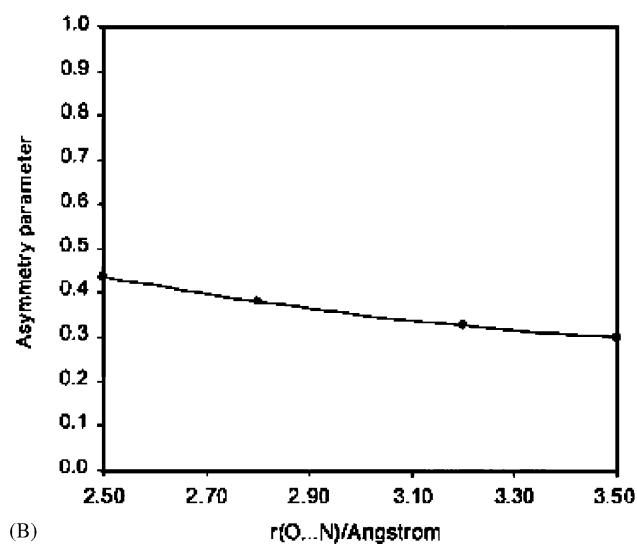
Fig. 9. Plots of the e^2qQ/h against the $\text{N}\cdots\text{O}$ separation ($R(\text{N}\cdots\text{O})$) (adapted from the latest data presented in [13,14,39]).

general geometry of the local environment (i.e. secondary structure) has also to be taken into consideration. In poly(L-alanine), the α -helix and β -sheet forms show a difference in δ_{iso} of 33 ppm, which is related to the different hydrogen bonding of these two different secondary structures [13].

Solid-solid NMR has been used to study short strong hydrogen bonds (SSHB or LBHB for low barrier hydrogen bonds), which can contribute up to 20 kcal/mol stabilization to transition states. With a bond length of ~ 2.4 Å, lithium hydrogen phthalate monohydrate is a SSHB ($\text{O}\cdots\text{O}$ distance = 2.4 Å). Its MAS spectrum provides strong evidence for a SSHB due to a low isotropic chemical shift, with lowest reported for a



(A)



(B)

Fig. 10. Calculated ^{17}O quadrupole coupling constant (A) and asymmetry parameter (B) versus $R(\text{O}\cdots\text{N})$ for the *N*-methylacetamide/formamide model (adapted from [62] with permission of the copyright owner).

carboxylate (46 ppm) [82]. Therefore, ^{17}O solid-state NMR can be easily used for identifying low barrier hydrogen bonds. This shows again that quadrupole interaction and chemical shift are strongly affected by hydrogen bonding.

Recently, Wu et al. [79] provided a comprehensive ^{17}O NMR study on potassium hydrogen benzoate. One of its interesting features is a single O–H–O symmetric hydrogen bond. Extensive simulation using both HF and DFT investigated the effect of such a symmetrical hydrogen bond on the ^{17}O NMR parameters. With the O–O distance 2.51 Å here, the isotropic chemical shift observed is much larger than that for lithium hydrogen phthalate.

Nuclear quadrupole resonance (NQR) is an alternative technique that can be used to characterize ^{17}O -labelled organic molecules and study the effect of hydrogen-bonding on the ^{17}O electric field gradient tensor [54,55] (see Table 3). Poplett and co-workers studied hydrogen-bonding in carboxylic acids and were the first to notice a dependence between components of the quadrupole coupling tensor and the hydrogen-bond length [50–52]. Seliger [55] has proposed using the principal value V_{33} of the electric field gradient tensor as a parameter reflecting the hydrogen bond strength. In the case of organic solids containing C–O–H \cdots O=C hydrogen bonds, Seliger has shown that it is possible to build a simple model to correlate V_{33} with the length $R(\text{O}\cdots\text{O})$ between the two oxygen atoms involved in the bond (Fig. 11). This correlation is based on several assumptions that include (1) that the electric field gradient tensor at the oxygen sites is mainly of a relatively local nature, (2) that the electron distribution around the hydrogen nucleus is reflected in the principal value V_{33} of the EFG tensor along the out-of-plane principal direction which is perpendicular to the oxygen–hydrogen bond, and (3) that no violent thermal motions are significantly influencing the ^{17}O EFG tensor (librations, reorientations, hydrogen exchange, etc.). If the EFG tensor is partially averaged due to the thermal motions the correlation becomes invalid. Therefore, this empirical correlation works only at a low enough temperature so that the influence of thermal motions on the EFG tensor can be neglected. Interestingly, the parameters obtained from potassium hydrogen benzoate [79] fit Seliger's correlation for the hydrogen bond length.

With the exception of one report [117], the effects of the temperature on the quadrupole coupling constant has not been studied in organic molecules. By observing the effects of the temperature on the static ^{17}O solid-state NMR spectrum of a single-crystal, Filsinger and co-workers characterized a motional process in hydrogen-bonded dimethylmalonic acid, suggesting 180°-flips of the $(\text{COOH})_2$ units. NQR studies have shown that the temperature has non-negligible effects on the values of

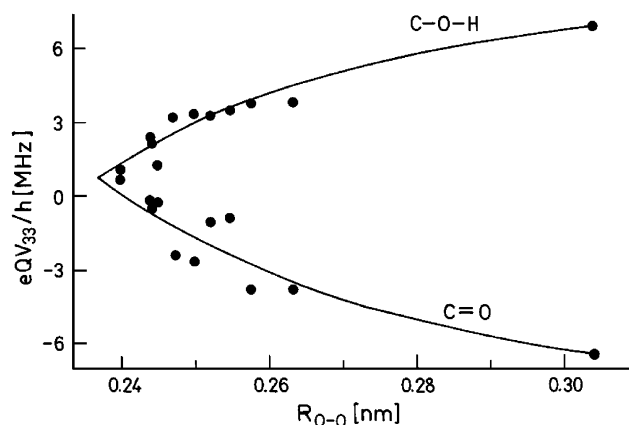


Fig. 11. Empirical expression giving a reasonable description of the correlation V_{33} vs. $R(\text{O}\cdots\text{O})$ in the range $0.24 \text{ nm} < R(\text{O}\cdots\text{O}) < 0.3 \text{ nm}$. The plot of eQV_{33}/h at the C– ^{17}O –H and C= ^{17}O –H oxygen sites versus the hydrogen bond length $R(\text{O}\cdots\text{O})$. The full lines are calculated after: $V_{33}(\text{C}–\text{O}–\text{H}) = 9.5 \text{ MHz} - 27 \text{ MHz } R_{\text{O}\cdots\text{O}}^{-3} - 1290 \text{ MHz } R_{\text{O}\cdots\text{O}}^{-6}$, $V_{33}(\text{C}=\text{O}) = -10.2 \text{ MHz} + 56 \text{ MHz } R_{\text{O}\cdots\text{O}}^{-3} + 1400 \text{ MHz } R_{\text{O}\cdots\text{O}}^{-6}$, where the hydrogen bond distances is given in 0.1 nm (adapted from [55] with permission of the copyright owner).

the quadrupole coupling constants and the quadrupolar asymmetry parameters [50,54]. In principle, variable temperature NMR and changes in the lineshape could be related to motion, although for many of the line shapes so far observed at room temperature there is little direct evidence of any effects of motion.

Studies of ^{17}O magnetic resonance in organic molecules have highlighted the complex dependence between the ^{17}O NMR parameters and molecular structure. The general conclusion is that EFG and chemical shift tensors are very sensitive to hydrogen bonding and can therefore be used to characterize such interactions. Several empirical correlations [39,40,55,62] matching some ^{17}O NMR parameters and the hydrogen bond length indicate that for some subset of molecules (or subset of hydrogen bonds) there is a relation between several of the ^{17}O NMR parameters and the hydrogen bond length, but these will need to be developed further.

6.5. Inorganic ^{17}O -labelled molecules bound to proteins and bilayers

6.5.1. O_2 and CO as ligands of hemeproteins

Heme model compounds and hemeproteins have been extensively studied by ^{17}O solution NMR [118–124] and, only more recently, ^{17}O solid-state NMR has also been used to provide structural data on such systems.

Since the first determination in 1991 of the ^{17}O NMR parameters from a C^{17}O molecule bound to a model compound for heme protein (a “picket fence porphyrin”) in the solid-state [123] (a spinning speed of only

4.7 kHz—resulted in many spinning side-bands), the quality of the spectra has increased and solid-state NMR has provided information about the conformation of not only bound-CO but also bound-O₂ in heme models and metalloproteins.

Oldfield et al. [125] studied a model compound for oxyhemoglobin and oxymyoglobin, the iron–dioxygen complex of “picket fence porphyrin” using ¹⁷O solid-state NMR. It was possible to determine the ¹⁷O NMR parameters (chemical shift tensor and nuclear quadrupole coupling constant) for all the oxygen sites from the porphyrin-bound O₂ molecule. Comparison with previous solution studies [124] showed observable changes in the NMR parameters. An estimation of the Fe–O–O bond angle (140°) for the model system was possible using the partial averaging of the shift tensor at room temperature. Temperature dependences indicate no changes in isotropic chemical shift for terminal oxygen while there is a low-frequency shift for the bridging oxygen—interpreted as the freezing of the system in one conformational substate. The nuclear quadrupole coupling constants are small when compared to O₃, suggesting a π -delocalization on the Fe–O–O fragment. Oxymyoglobin and oxyhemoglobin themselves could also be observed in frozen solution, showing spectra similar to the model porphyrin.

Since 1998, two studies of metalloporphyrins and metalloproteins, using simultaneously ¹³C and ¹⁷O solid-state NMR, ⁵⁷Fe Mössbauer and infrared vibrational spectroscopic techniques, and DFT quantum simulation to probe various Fe–O₂ or Fe–CO conformations, have provided accurate structural information on the conformation of the bound molecules relative to the Fe centre. McMahon et al. [113] studied how a CO ligand binds to iron in metalloporphyrins and metalloproteins (extending Park et al.’s work that was mainly focused on the use of ¹⁷O solution NMR [123]). This approach using DFT to test several models against the spectroscopic data, was the first detailed quantum chemical analysis of metal–ligand geometries in metalloproteins, and has allowed the determination of the most probable ligand tilt and bend angles. This is a useful complement to X-ray diffraction, where the resolution on the ligand (CO) could not sufficiently constrain its orientation [113] (resulting in a large distribution of angles from one crystal structure to another). This study shows that all spectroscopic methods taken together converge to a single conformation, very close to linear and untilted Fe–C–O geometry for all carbonmonoxyheme proteins. The same approach was applied to study several Fe–O₂ analogue metalloporphyrins [126]. NMR results are well reproduced by DFT, enabling testing of various models of Fe–O₂ bonding in the porphyrin and metalloproteins. No evidence was found for two binding sites in an oxypicket fence porphyrin. Oxygen sites in complexes are more electronegative than that in the CO system,

which strongly supports the idea that H-bonding to O₂ is a major contributor to O₂/CO discrimination in heme proteins.

6.5.2. Molecules of water interacting with bilayers

Bilayers are by their very nature at the border between liquid and solids. Water molecules, which constitute an important part of such lyotropic phases, experience an anisotropic environment through the interactions with the bilayers and thus anisotropic molecular motions, resulting in the quadrupolar interaction not being averaged out to zero. Tricot et al. [127] compared ¹⁷O and ²H NMR spectra of water (both ²H₂O and H₂¹⁷O) in fully hydrated lamellar phase of DPPC (dipalmitoylphosphatidylcholine). Ordering of water molecule results in a quadrupolar splitting which is related to the order parameter. In the case of ¹⁷O, the quadrupolar splitting observed is larger than for ²H.

7. Future prospects

7.1. Use of ¹⁷O as a probe for drug-receptor interaction

Several of the organic molecules studied as crystals also have other properties, such as interacting with one or several receptors or enzymes. Providing that ¹⁷O solid-state NMR has sufficient sensitivity (i.e. high magnetic field and high ¹⁷O enrichment) to measure a signal, it should be possible to characterize the local electronic environment sensed by the ¹⁷O labels of such molecules while interacting at the binding site/pocket of the protein. Information relative to the protonation-state of the bond–ligand could also be provided. Of course, information on the existence of hydrogen-bonds between the ligand and a qualitative picture of the strength of the hydrogen-bonds involved could also be available.

7.2. Distance measurements: measuring distances between ¹H–¹⁷O and ¹³C–¹⁷O nuclei

There has been very little work using ¹⁷O NMR to determine distance. Linder et al. have indicated the possibility of correlating the quadrupole and dipole tensor by quadrupole separated local field experiments on powder samples [128]. This has been applied to the ¹H–¹⁷O system in Mg(OH)₂ and Mg(OH)_x(OCH₃)_{2–x} [129]. Lee–Goldburg decoupling during the dipolar evolution provides better resolution in the dipolar dimension. The normal chemical shift dimension produces the second-order quadrupolar lineshape and the dipolar dimension allows the dipolar interaction to be calculated. The 2D data contain more information since the intensity distribution depends critically on the relative orientation of the two tensors. Since the dipolar

interaction is axially symmetric, only the azimuthal and polar angles are necessary to describe the relative orientation, and the intensity distribution changes markedly with this orientation (Fig. 12).

In 2003, Hu et al. [130] presented the application of a 2D static NMR experiment (Fig. 13) to provide a good approximation of the ^1H – ^{17}O distance in ice at 90 K. To allow ready interpretation of the static experiment, it is best applied to systems with a single ^1H – ^{17}O bond or hydrogen bond. The method could in principle be applied to α -helix forming transmembrane peptides in which a single ^{17}O -labelled amino acid has been inserted and providing a single ^1H – ^{17}O hydrogen bond (Fig. 14). This approach might be able to focus on local deformation of the helix induced by the membrane.

Developing robust MAS or DOR pulse sequences which allow the selective reintroduction of the dipolar interaction in order to measure distances between a ^{17}O nucleus and another nucleus of interest will be a very important step forward. REDOR and REAPDOR have already been demonstrated in the case of ^{13}C – ^{17}O internuclear distances [131] for ^{17}O labelled water co-crystallized with L-asparagine and other $S = 1$, $I = \frac{1}{2}$ I – S internuclear distances [132]. Obviously more work in this direction should be carried out in order to have robust methodologies that can be applied to biological samples. Cross-polarisation (CP) can also be used to discriminate different sites as those with the protons in closer proximity cross-polarize more strongly at shorter contact times. This principle has been illustrated for ^1H – ^{17}O for both conventional CP and generation of multiple quantum signal [133,134].

With the demonstration that ^{17}O solid-state NMR provides enough sensitivity to study selectively enriched peptides in a non-crystalline phase or inserted in vesicles, the development of efficient pulses sequences to measure internuclear distances between pairs of nuclei including an ^{17}O , should be the next logical step in order to realise the full potential of the technique.

7.3. Synthetic challenges

Not all the chemical functionalities involving oxygen are equally amenable to ^{17}O enrichment. For carboxylic groups, the exchange is relatively straightforward. Other chemical groups, like alcohol are more difficult to enrich and therefore much less common in the literature.

Synthesis of selectively enriched peptides is possible and is also compatible with solid-phase peptide synthesis [42]. However, the techniques used for peptide synthesis prevent the insertion of ^{17}O labels in the side-chains of the amino acids, due to the chemical protection required for the synthesis to take place. Currently, the only way available to synthesize a peptide with ^{17}O -labelled side-chains would consist of adding a supplementary ^{17}O -enrichment step after purification of the peptide,

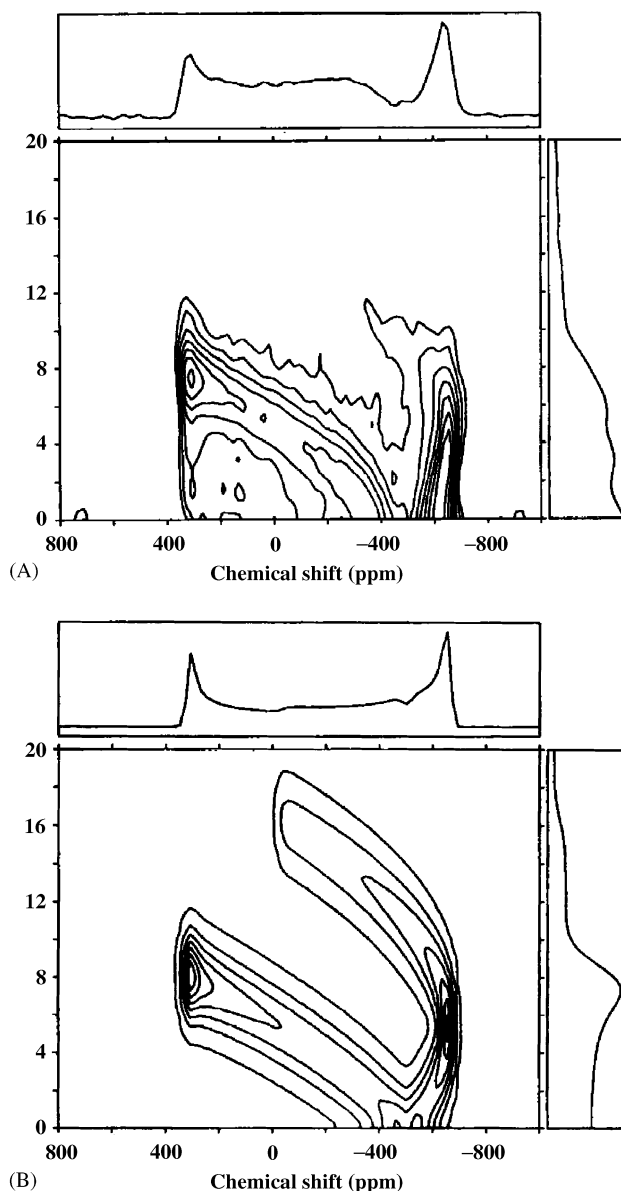


Fig. 12. A quadrupole–dipole separated local field experiment for the OH group in $\text{Mg}(\text{OH})_x(\text{OCH}_3)_{2-x}$ with (A) the experimental data compared with (B) the simulation of the intensity assuming the tensors are collinear from van Eck and Smith [129] with permission of the copyright owner.

increasing even more the cost of the sample. The preparation of such a sample has not yet been reported.

8. Conclusions

NMR of ^{17}O -labelled biomaterials is very sensitive to changes in the local bonding environment. Indeed, the chemical shift and quadrupole coupling constant change significantly in different protonation states of the same molecule or very similar molecules forming slightly different crystal forms.

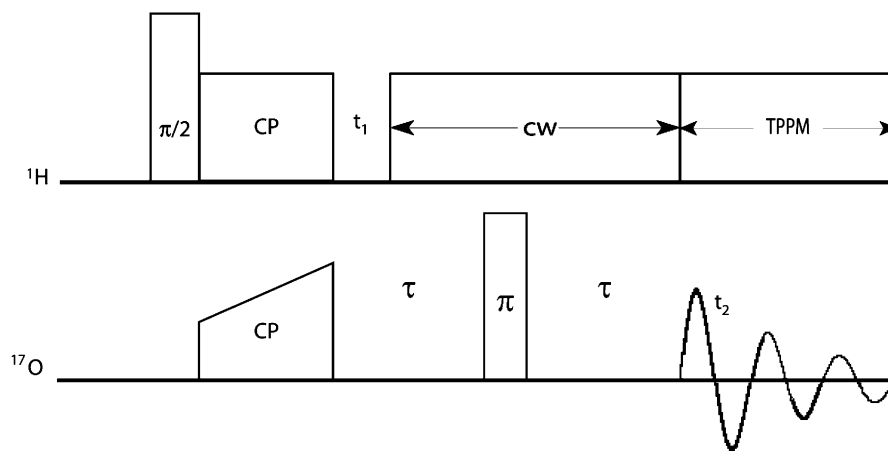


Fig. 13. CP-Echo pulse sequence applied to a glycerol ^{17}O -water by Hu et al.[130] in order to estimate the average O–H distance in ice.

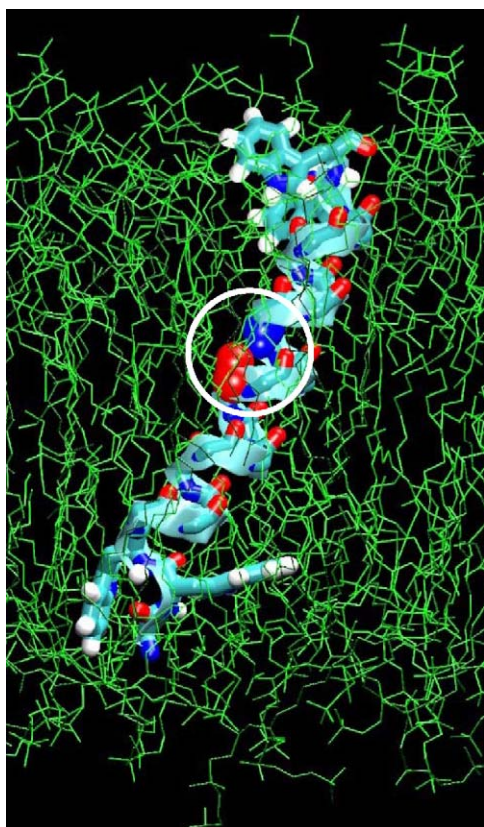


Fig. 14. Example where a dipole–quadrupole correlation 2D static NMR experiment could be applied on a biological sample.

The ability to resolve the different sites and to detect subtle bonding changes through ^{17}O NMR spectra suggests it has potential to become one of the most significant probe techniques for biochemical investigation of ligand–receptor interactions as it is a non-perturbing approach. Furthermore, molecular size is in principle not a limiting factor for spectral resolution

(which differs from solution). Although much of the methodology in this review (e.g. MAS) is not limited by crystallinity, the ultimate resolution achievable (via DOR, MQMAS, STMAS) depends sensitively on the microcrystallinity.

Acknowledgments

The authors would like to acknowledge Ray Dupree's central contribution, continued interest and guidance in developing ^{17}O as a useful and informative nucleus for application to biology for which he has collaborated with us. V.L. thanks BBSRC for Industrial CASE Scholarship. The BBSRC, MRC, EPSRC and HEFCE are acknowledged for their support to A.W. for this work. A.W. was in receipt of a Professerial Research Fellowship, BBSRC. M.E.S. thanks EPSRC, HEFCE and the University of Warwick for supporting NMR equipment at Warwick and the Royal Society and Leverhulme Trust for a senior fellowship permitting him to start work on ^{17}O NMR in organic materials.

References

- [1] P.J. Dirken, M.E. Smith, H.J. Whitfield, *J. Phys. Chem.* 99 (1995) 395–401.
- [2] R. Hussin, D. Holland, R. Dupree, *J. Non-Cryst. Solids* 234 (1998) 440–445.
- [3] K.J.D. MacKenzie, M.E. Smith, *Multinuclear Solid State NMR of Inorganic Materials*, Pergamon Press, Oxford, 2002.
- [4] P.J. Dirken, S.C. Kohn, M.E. Smith, E.R.H. van Eck, *Chem. Phys. Lett.* 266 (1997) 568–574.
- [5] S.K. Lee, J.F. Stebbins, *J. Phys. Chem. B* 104 (2000) 4091–4100.
- [6] J.F. Stebbins, J.V. Oglesby, S. Kroeker, *Am. Mineral.* 86 (2001) 1307–1311.
- [7] L.S. Du, J.F. Stebbins, *J. Phys. Chem. B* 107 (2003) 10063–10076.

- [8] L.M. Bull, A.K. Cheetham, A. Samoson, T. Anupöld, A. Reinhold, J. Sauer, B. Bussemer, V. Moravetski, Y.K. Lee, S.L. Gann, J. Shore, A. Pines, R. Dupree, *J. Am. Chem. Soc.* 120 (1998) 3510–3511.
- [9] L.M. Bull, B. Bussemer, T. Anupöld, A. Reinhold, A. Samoson, J. Sauer, A.K. Cheetham, R. Dupree, *J. Am. Chem. Soc.* 122 (2000) 4948–4958.
- [10] S. Schramm, E. Oldfield, *J. Am. Chem. Soc.* 106 (1984) 2502–2506.
- [11] S.E. Ashbrook, A.J. Berry, S. Wimperis, *J. Phys. Chem. B* 106 (2002) 773–778.
- [12] S.E. Ashbrook, A.J. Berry, S. Wimperis, *J. Am. Chem. Soc.* 123 (2001) 6360–6366.
- [13] K. Yamauchi, S. Kuroki, I. Ando, T. Ozaki, A. Shoji, *Chem. Phys. Lett.* 302 (1999) 331–336.
- [14] K. Yamauchi, S. Kuroki, I. Ando, *J. Mol. Struct.* 602–603 (2002) 171–175.
- [15] G. Wu, *Biochem. Cell. Biol.* 76 (1998) 429–442.
- [16] W.W. Cleland, M.M. Kreevoy, *Science* 264 (1994) 1887.
- [17] K. Lee, W.A. Anderson, in: R.C. Weast, M.J. Astle, (Eds.), *CRC Handbook of Chemistry and Physics*, CRC Press, Boca Raton, 1980, pp. E70.
- [18] M.E. Smith, E.R.H. van Eck, *Prog. NMR Spectrosc.* 34 (1999) 159–201.
- [19] I.P. Gerathanassis, in: D. Grant, R.K. Harris (Eds.), *Encyclopedia of NMR*, Vol. 5, Wiley, New York, 1995, pp. 3430–3440.
- [20] D. Freude, in: R. Meyers (Ed.), *Encyclopedia of Analytical Chemistry*, Wiley, Chichester, 2000, pp. 12188–12224.
- [21] K.D. Kopple, *Biopolymers* 20 (1981) 1913–1920.
- [22] A. Abragam, *Principles of Nuclear Magnetism*, Clarendon Press, Oxford, 1961.
- [23] S. Dong, K. Yamada, G. Wu, *Z. Naturforsch.* 55a (2000) 21–28.
- [24] R. Goc, E. Ponnusamy, J. Tritt-Goc, D. Fiat, *Int. J. Pept. Protein. Res.* 31 (1988) 130–136.
- [25] H. Behrens, B. Schnabel, *Physica B* 114 (1982) 185–190.
- [26] A. Samoson, E. Lippmaa, A. Pines, *Mol. Phys.* 65 (1988) 1013–1018.
- [27] Y. Wu, B.Q. Sun, A. Pines, A. Samoson, E. Lippmaa, *J. Magn. Reson.* 89 (1990) 297–309.
- [28] A. Samoson, E. Lippmaa, *J. Magn. Reson.* 84 (1989) 410–416.
- [29] K.T. Mueller, B.Q. Sun, G.C. Chingas, J.W. Zwanziger, T. Terao, A. Pines, *J. Magn. Reson.* 86 (1990) 470–487.
- [30] A. Llor, J. Virlet, *Chem. Phys. Lett.* 152 (1988) 248–253.
- [31] L. Frydman, J.S. Harwood, *J. Am. Chem. Soc.* 117 (1995) 5367–5368.
- [32] Z. Gan, *J. Am. Chem. Soc.* 122 (2000) 3242–3243.
- [33] S.E. Ashbrook, S. Wimperis, *J. Magn. Reson.* 156 (2002) 269–281.
- [34] G. Wu, S. Dong, *J. Am. Chem. Soc.* 123 (2001) 9119–9125.
- [35] V. Lemaître, K.J. Pike, A. Watts, T. Anupöld, A. Samoson, M.E. Smith, R. Dupree, *Chem. Phys. Lett.* 371 (2003) 91–97.
- [36] A.E. Bennett, C.M. Rienstra, M. Auger, K.V. Lakshmi, R.G. Griffin, *J. Chem. Phys.* 103 (1995) 6951–6958.
- [37] D. Freude, J. Kärger, in: F. Schüth, K.S.W. Sing, J. Weitkamp, (Eds.), *Handbook of Porous Solids*, Vol. 1, Wiley-VCH, Weinheim, (2002), pp. 465–504.
- [38] R. Kuroki, I. Ando, A. Shoji, T. Ozaki, *Chem. Commun.* (1992) 433–434.
- [39] S. Kuroki, A. Takahashi, I. Ando, A. Shoji, T. Ozaki, *J. Mol. Struct.* 323 (1994) 197–208.
- [40] N. Asakawa, T. Kameda, S. Kuroki, H. Kurosu, S. Ando, I. Ando, A. Shoji, *Annu. Rep. NMR Spectrosc.* 35 (1998) 55–137.
- [41] L.G. Butler, in: D. Boykin, (Ed.), ¹⁷O NMR in Organic Chemistry, CRC Press, Boca Raton, (1991), pp. 1–19.
- [42] A. Steinschneider, M.I. Burgar, A. Buku, D. Fiat, *Int. J. Pept. Protein Res.* 18 (1981) 324–333.
- [43] A. Steinschneider, D. Fiat, *Int. J. Pept. Protein Res.* 23 (1984) 591–600.
- [44] B. Valentine, A. Steinschneider, D. Dhawan, M.I. Burgar, T. St Amour, D. Fiat, *Int. J. Pept. Protein Res.* 25 (1985) 56–68.
- [45] K.J. Pike, V. Lemaître, A. Kukol, T. Anupöld, A. Samoson, A.P. Howes, A. Watts, M.E. Smith, R. Dupree, *J. Phys. Chem. B*, in press.
- [46] J.A. Jackson, *J. Phys. Chem.* 24 (1963) 591.
- [47] W. McFarlane, C.E. McFarlane, in: J. Mason (Ed.), *Multi-nuclear NMR*, Plenum Press, New York, 1987.
- [48] H.A. Christ, P. Diehl, H.R. Schneider, H. Dahn, *Helv. Chem. Acta* 44 (1961) 865.
- [49] C.P. Cheng, T.L. Brown, *J. Am. Chem. Soc.* 101 (1979) 2327–2334.
- [50] S.G.P. Brosnan, D.T. Edmonds, I.J.F. Poplett, *J. Magn. Reson.* 45 (1981) 451–460.
- [51] I.J.F. Poplett, J.A.S. Smith, *J. Chem. Soc. Faraday Trans.* 277 (1981) 1473–1485.
- [52] I.J.F. Poplett, M. Sabir, J.A.S. Smith, *J. Chem. Soc. Faraday Trans.* 277 (1981) 1651–1668.
- [53] J. Seliger, V. Zagar, R. Blinc, P.K. Kadaba, *Z. Naturforsch.* 45a (1990) 733–735.
- [54] J. Seliger, V. Zagar, *Chem. Phys.* 234 (1998) 223–230.
- [55] J. Seliger, *Chem. Phys.* 231 (1998) 81–86.
- [56] S. Dong, R. Ida, G. Wu, *J. Phys. Chem. A* 104 (2000) 11194–11202.
- [57] G. Wu, K. Yamada, A. Dong, H. Grondey, *J. Am. Chem. Soc.* 122 (2000) 4215–4216.
- [58] C.J. Pickard, F. Mauri, *Phys. Rev. B. Condens. Matter* 63 (2001) 245101–245113.
- [59] M. Profeta, F. Mauri, C.J. Pickard, *J. Am. Chem. Soc.* 125 (2003) 541–548.
- [60] J.R. Yates, C.J. Pickard, M.C. Payne, R. Dupree, M. Profeta, F. Mauri, *J. Phys. Chem. B*, submitted.
- [61] R. Goc, J. Tritt-Goc, D. Fiat, *Bull. Magn. Reson.* 11 (1989) 238–243.
- [62] K. Yamada, S. Dong, G. Wu, *J. Am. Chem. Soc.* 122 (2000) 11602–11609.
- [63] G. Wu, S. Dong, R. Ida, N. Reen, *J. Am. Chem. Soc.* 124 (2002) 1768–1777.
- [64] G. Wu, S. Dong, R. Ida, *Chem. Commun.* (2001) 891–892.
- [65] A. Takahashi, S. Kuroki, I. Ando, T. Ozaki, A. Shoji, *J. Mol. Struct.* 442 (1998) 195–199.
- [66] W. Scheubel, H. Zimmermann, U. Haeberlen, *J. Magn. Reson.* 63 (1985) 544–555.
- [67] E.B. Fleischer, N. Sung, S. Hawkinson, *J. Phys. Chem.* 72 (1968) 4311–4312.
- [68] Q. Gao, G.A. Jeffrey, J.R. Ruble, R.K. McMullan, *Acta Crystallogr. Sec. B* 47 (1991) 742–745.
- [69] S. Kashio, K. Ito, M. Haisa, *Bull. Chem. Soc. Jpn.* 52 (1979) 365.
- [70] L. Leiserowitz, M. Tuval, *Acta Crystallogr. Sec. B* 34 (1978) 1230–1247.
- [71] S.W. Johnson, J. Eckert, M. Barthes, R.K. McMullan, M. Muller, *J. Phys. Chem.* 99 (1995) 16253–16260.
- [72] F. Iwasaki, Y. Kawano, *Acta Crystallogr. Sec. B* 34 (1978) 1286–1290.
- [73] P. Coppens, G.M. Schmidt, *Acta Crystallogr.* 18 (1965) 62–67.
- [74] A. Mostad, C. Rummung, *Chem. Acta Scand.* 27 (1973) 401.
- [75] Q. Zhang, E.Y. Chekmenev, R.J. Wittebort, *J. Am. Chem. Soc.* 125 (2003) 9140–9146.
- [76] T.M. Sabine, G.W. Cox, B.M. Craven, *Acta Crystallogr. Sec. B* B25 (1969) 2437–2441.
- [77] G.A. Sim, J.M. Robertson, T.H. Goodwin, *Acta Crystallogr.* 8 (1955) 157–164.

- [78] J.M. Skinner, G.M.D. Stewart, J.C. Speakman, *J. Chem. Soc.* (1954) 180.
- [79] G. Wu, K. Yamada, *Solid State Nucl. Magn. Reson.* 24 (2003) 196–208.
- [80] G. Wu, S. Dong, R. Ida, N. Reen, *J. Am. Chem. Soc.* 124 (2001) 1768–1777.
- [81] I.A. Oxtton, T.S. Cameron, O. Knop, A.W. McCulloch, *Can. J. Chem.* 55 (1977) 3831.
- [82] A.P. Howes, R. Jenkins, M.E. Smith, D.H.G. Crout, R. Dupree, *Chem. Commun.* (2001) 1448–1449.
- [83] W. Nowacki, H. Jaggi, *Z. Crystallogr.* 109 (1957) 272.
- [84] H. Küppers, F. Takusagawa, T.F. Koetzle, *J. Phys. Chem.* 82 (1985) 5636.
- [85] Y. Okaya, *Acta Crystallogr.* 19 (1965) 879.
- [86] S.K. Arora, M. Sundaralingam, *Acta Crystallogr. Sec. B* 27 (1971) 1293–1298.
- [87] A.W. Pryor, P.L. Sanger, *Acta Crystallogr. Sec. B* 26 (1970) 543–558.
- [88] S. Swaminathan, B.M. Craven, R.K. McMullan, *Acta Crystallogr. Sec. B* 40 (1984) 300–306.
- [89] D.L. Barker, R.E. Marsh, *Acta Crystallogr.* 17 (1964) 1581–1587.
- [90] R.J. McClure, B.M. Craven, *Acta Crystallogr. Sec. B* 29 (1973) 1234–1238.
- [91] U. Thewalt, C.E. Bugg, R.E. Marsh, *Acta Crystallogr. Sec. B* 27 (1971) 2358–2363.
- [92] K. Ozeki, N. Sakabe, J. Tanaka, *Acta Crystallogr. Sec. B* 25 (1969) 1038–1045.
- [93] R.F. Stewart, L.H. Jensen, *Acta Crystallogr.* 23 (1967) 1102–1105.
- [94] M. Lehmann, T. Koetzle, W. Hamilton, *J. Cryst. Mol. Struct.* 2 (1972) 225–233.
- [95] S.L. Gann, J.H. Baltisberger, E.W. Wooten, H. Zimmermann, A. Pines, *Bull. Magn. Reson.* 16 (1994) 68–72.
- [96] B. di Blasio, V. Pavone, C. Pedone, *Cryst. Struct. Comm.* 6 (1977) 745.
- [97] A. Sequeira, H. Rajagopal, R. Chidambaram, *Acta Crystallogr. B* 28 (1972) 2514–2519.
- [98] C. Sano, N. Nagashima, T. Kawakita, Y. Iitaka, *Anal. Sci.* 5 (1989) 121–122.
- [99] N. Shamala, K. Venkatesan, *Cryst. Struct. Commun.* 1 (1972) 227.
- [100] A.R. Al-Karaghoul, T.F. Koetzle, *Acta Crystallogr. Sec. B* 31 (1975) 2461–2465.
- [101] M.N. Frey, T.F. Koetzle, M.S. Lehmann, W.C. Hamilton, *J. Chem. Phys.* 58 (1973) 2547–2556.
- [102] T.F. Koetzle, L. Golic, M.S. Lehmann, J.J. Verbist, W.C. Hamilton, *J. Chem. Phys.* 60 (1974) 4690–4696.
- [103] A. Kevick, A.R. Al-Karaghoul, T.F. Koetzle, *Acta Crystallogr. Sec. B* 33 (1977) 3796–3801.
- [104] N.S. Rao, R. Parthasarathy, *Acta Crystallogr. Sec. B* 29 (1973) 2379–2388.
- [105] W.T. Astbury, C.H. Dalglish, S.E. Darmon, G.B.B.M. Sutherland, *Nature* 69 (1948) 780.
- [106] F.H.C. Crick, A. Rich, *Nature* 176 (1955) 780.
- [107] H. Saito, I. Ando, *Annu. Rep. NMR Spectrosc.* (1989) 210.
- [108] S. Arnott, A.L. Wonacott, *J. Mol. Bio.* 21 (1966) 371.
- [109] S. Arnott, S.D. Dover, A.J. Elliot, *J. Mol. Bio.* 30 (1967) 201.
- [110] G. Wu, A. Hook, S. Dong, K. Yamada, *J. Phys. Chem. A* 104 (2000) 4102–4107.
- [111] Q.W. Zhang, H.M. Zhang, M.G. Usha, R.J. Wittebort, *Solid State Nucl. Magn. Reson.* 7 (1996) 147–154.
- [112] T.M. Sabine, G.W. Cox, B.M. Craven, *Acta Crystallogr. Sec. B* 25 (1969) 2437–2441.
- [113] M.T. McMahon, A.C. deBios, N. Godbout, R. Salzmänn, D.D. Laws, H. Le, R.H. Havlin, E. Oldfield, *J. Am. Chem. Soc.* 120 (1998) 4784–4797.
- [114] C.G. Suresh, M. Vijayan, *Int. J. Pept. Protein. Res.* 22 (1983) 129–143.
- [115] S. Kuroki, S. Ando, I. Ando, *Chem. Phys.* 195 (1995) 107–116.
- [116] G.A. Jeffrey, *An Introduction to Hydrogen Bonding*, Oxford University Press, New York, 1997.
- [117] B. Filsinger, H. Zimmermann, U. Haeberlen, *Mol. Phys.* 76 (1987) 6944.
- [118] H.C. Lee, K. Cummings, K. Hall, L.P. Hager, E. Oldfield, *J. Bio. Chem.* 263 (1988) 16118–16124.
- [119] H.C. Lee, E. Oldfield, *J. Am. Chem. Soc.* 111 (1989) 1584–1590.
- [120] I.P. Gerothanassis, *Prog. NMR Spectrosc.* 26 (1994) 239.
- [121] I.P. Gerothanassis, M. Momenteau, *J. Am. Chem. Soc.* 109 (1987) 6944.
- [122] I.P. Gerothanassis, B. Looock, M. Momenteau, *Chem. Commun.* (1992) 598.
- [123] K.D. Park, K.M. Guo, F. Adebodun, M.L. Chiu, S.G. Sligar, E. Oldfield, *Biochemistry* 30 (1991) 2333–2347.
- [124] I.P. Gerothanassis, M. Momenteau, B. Looock, *J. Am. Chem. Soc.* 111 (1989) 7006–7012.
- [125] E. Oldfield, H.C. Lee, C. Coretsopoulos, F. Adebodun, K.D. Park, J. Chung, B. Philips, *J. Am. Chem. Soc.* 113 (1991) 8680–8685.
- [126] N. Godbout, K.L. Sanders, R. Salzmänn, R.H. Havlin, M. Wojdelski, E. Oldfield, *J. Am. Chem. Soc.* 121 (1999) 3829–3844.
- [127] Y. Tricot, W. Niederberger, *Biophys. J.* 9 (1979) 195–200.
- [128] M. Lindner, A. Höhener, R.R. Ernst, *J. Phys. Chem.* 73 (1980) 4959.
- [129] E.R.H. van Eck, M.E. Smith, *J. Chem. Phys.* 108 (1998) 5904–5912.
- [130] K.N. Hu, D. Iuga, R.G. Griffin, in: 44th Experimental NMR Conference, Savannah, USA, 2003, 198.
- [131] L. Chopin, S. Vega, T. Gullion, *J. Am. Chem. Soc.* 120 (1998) 4406–4409.
- [132] E.T. Hughes, T. Gullion, A. Goldbourt, S. Vega, A.J. Vega, *J. Magn. Reson.* 156 (2002) 230–241.
- [133] T.H. Walter, G.L. Turner, E. Oldfield, *J. Magn. Reson.* 76 (1988) 106–120.
- [134] S.E. Ashbrook, S. Wimperis, *J. Magn. Reson.* 147 (2000) 238–249.